STATISTICAL VALIDATION OF A NUMERICAL SNOW COVER MODEL AND PRELIMINARY EXPERIMENTAL RESULTS TO FACILITATE MODEL IMPROVEMENT

by

Christopher Charles Lundy

A thesis submitted in partial fulfillment
of the requirements for the degree

of

Master of Science

in

Civil Engineering

MONTANA STATE UNIVERSITY
Bozeman, Montana

July 2000

APPROVAL

of a thesis submitted by

Christopher Charles Lundy

This thesis has been read by each member of the thesis committee and has been found to be satisfactory regarding content, English usage, format, citations, bibliographic style, and consistency, and is ready for submission to the College of Graduate Studies.

Dr. Robert Brown _____ _____
(Signature) (Date)

APPROVED FOR THE DEPARTMENT OF CIVIL ENGINEERING

Dr. Donald Rabern _____ _____
(Signature) (Date)

APPROVED FOR THE COLLEGE OF GRADUATE STUDIES

Dr. Bruce McLeod _____ _____
(Signature) (Date)

STATEMENT OF PERMISSION TO USE

In presenting this thesis in partial fulfillment of the requirements for a master's degree at Montana State University, I agree that the Library shall make it available to borrowers under rules of the Library.

If I have my intention to copyright this thesis by including a copyright notice page, copying is allowable only for scholarly purposes, consistent with "fair use" as prescribed in the U.S. Copyright Law. Requests for permission for extended quotation from or reproduction of this thesis in whole or parts may be granted only by the copyright holder.

Signature_____

Date_____

TABLE OF CONTENTS

TABLE OF CONTENTS – CONTINUED

LIST OF TABLES

LIST OF FIGURES

LIST OF FIGURES – CONTINUED

Figure Page

LIST OF FIGURES – CONTINUED

Figure Page

ABSTRACT

A computer model called SNOWPACK has been developed by the Swiss Federal Institute for Snow and Avalanche Research that simulates the evolution of a mountain snowpack. Using meteorological parameters measured at mountain weather sites, a prediction of snowpack stratigraphy is made by modeling snow characteristics such as snow depth, temperature, density, grain size, and crystal type. In order to evaluate the accuracy of the model, SNOWPACK was run using meteorological variables measured at a mountain weather station near Bozeman, Montana, and weekly snow profiles were conducted to provide a benchmark for the model output. A statistical analysis was then performed in order to objectively compare the predicted snowpack to the snow profile data.

While kinetic-growth metamorphism has been investigated in the laboratory previously, new technologies allow similar experiments to be performed with greater accuracy and efficiency. A methodology was developed that utilizes a computed tomography (CT) scanner to obtain cross-sectional images over time of a snow sample under a large temperature gradient. Using innovative stereological software, the microstructural properties of the snow can then be measured from the two-dimensional CT images.

SNOWPACK predicts snowpack temperatures with reasonable accuracy, but is less effective at simulating density. Different definitions of grain size utilized by the model and human observers resulted in large variations between the modeled and observed grain size. Predicted and observed grain types also demonstrated low correlation. Other aspects of the analysis suggest that the manner in which the surface energy exchange, wet snow metamorphism, and new snow density are modeled need refinement. Despite these deficiencies, SNOWPACK still provides the snow practitioner with a useful tool for simulating the mountain snowpack. The laboratory experiments succeeded in quantifying the changes in snow microstructure during kinetic-growth metamorphism, but are also applicable to equilibrium conditions. The presented methodology demonstrates that CT technology and stereological methods are improvements over previous techniques for investigating snow metamorphism. Since the metamorphism laws in SNOWPACK are based on snow microstructure, the results of future experiments could provide data permitting validation and improvement of these theories.

CHAPTER 1

INTRODUCTION

Introduction to Snow Metamorphism

The seasonal snowpack found in alpine environments has been the subject of both observation and organized research since at least the early 1800s (Colbeck, 1991). Much of these studies have been conducted in an effort to better understand and predict the release of avalanches, which are a significant threat to both life and property in the mountainous regions throughout the world.

In most mountainous environments, snow blankets the ground for large portions of the year. Storms throughout the fall, winter, and spring deposit fresh snow which accumulates over time to create the seasonal snowpack. Since these snowfalls are often separated by periods of contrasting weather, such as sunny, warm periods, cold snaps, or high winds, the snowpack is often observed to have a stratified configuration (Seligman, 1936). It is on these layers that avalanches often initiate and slide.

Once on the ground, the snow creates a complex granular aggregate comprised of ice grains and interstitial pore space. The porous nature of the snowpack is of great consequence as it allows the transference of water, either as a vapor or liquid, within the material. Dry snow is a three-constituent material composed of the solid and vapor states

of water as well as air. If liquid water is present, as it often is during warmer periods of the winter and especially in the spring, the snow is classified as wet.

As soon as new snow lands on the snowpack, it begins a process of metamorphism that continues until it finally melts in the spring and summer. This phenomenon was first described in detail by Paulcke (1934), although it is commonly believed that the changes occurring within the seasonal snow pack have been observed since the 1800s. Metamorphic processes are complex and change the properties of the individual snow grain as well as its relation to the snow particles surrounding it. Snow crystals may become smaller or larger, change shape, and become more or less bonded to its neighboring grains. While similar metamorphic processes may be taking place in snow within a common horizontal layer, snow at different vertical levels will often be metamorphosing very differently. Frequently, this serves to further differentiate the successive layers of snow, intensifying the stratified structure of the snowpack. Other times, metamorphism causes portions of the snowpack to become more homogenous.

Types of Snow Metamorphism

Generally, two distinct metamorphic processes are recognized; the first is termed equilibrium metamorphism and is characterized by the production of smaller, rounded snow grains that are well-bonded to neighboring crystals. Snow that has undergone equilibrium metamorphism is typically strong and fairly dense. The second type of metamorphism results in weaker, larger-grained snow and has been termed kinetic-growth metamorphism. The resulting snow grains are angular, hexagonal, or faceted in

shape and often poorly bonded to surrounding snow particles. The extent of the intergranular bonding depends on the snow density, temperature, temperature gradient, and orientation of the bond relative to the temperature gradient.

The type and rate of metamorphism occurring within the layers of an alpine snowpack is dependent on several parameters, including the temperature, temperature gradient, overburden pressure, density, and crystal type of the snow layer. Of these factors, temperature gradient is the most critical in controlling which type of metamorphism dominates. Temperature gradients develop within the snow cover since the base of the snowpack in contact with the ground is held at a relatively constant 0 deg C due to stored summer heat, and the air temperature at the snow surface is often significantly colder. When the snowpack is deep and the ambient air temperature is warm, the temperature gradient within the snow cover will be small and equilibrium metamorphism will be the most prevalent. These conditions are common in coastal or maritime climate regimes. In the more inland, or continental, mountain ranges, the snowpack is typically shallow and the air temperature is colder. The result is higher temperature gradients which drive kinetic-growth metamorphism.

Overview of Kinetic-Growth Metamorphism

As a result of the large thermal differences within the snow cover, a gradient in vapor pressure forms so that water vapor diffuses within the snow pore space (Colbeck, 1983), a process which has been conceptualized for over forty years as the “hand-to-hand” delivery of water vapor (Yosida et al, 1955). This visualization conveniently

describes the fundamental process of kinetic-growth metamorphism: the sublimation of water vapor from a “source” grain and the subsequent vertical diffusion and condensation onto a “sink” grain. As the diffusion process continues, larger crystals tend to grow rapidly at the expense of smaller grains. The result of kinetic-growth metamorphism is, in the early stages, angular ice grains characterized by flat faces and sharp edges. As the crystals reach more advanced stages of development, the growth of the crystals become oriented normal to the slope; the resultant snow grains are typically hollow, striated columns or cups. In the final stage of the metamorphic process, the crystals become columnar with the c-axis oriented perpendicular to the sope. These new crystal types are often called faceted grains, temperature gradient (TG) snow, kinetic-growth forms, recrystallized snow, or depth hoar.

During the formation of faceted snow, water vapor can move through the snow pore space either by diffusion or convection. While diffusion is generally accepted as the dominant process during metamorphism, the role of convection has been subject to conjecture. Trabant and Benson (1972) calculated vapor fluxes that were an order of magnitude higher than those predicted by early diffusion-only models (Bader, 1939; Giddings and LaChapelle, 1962). They attributed these higher rates to convection within the snowpack. However, these differences have been attributed to faults in the early models by Colbeck (1980), who points out that the one-dimensional diffusive vapor flow equations used by previous models can significantly underestimate the vapor flux. Experiments conducted by Akitaya (1974) demonstrated that convection was likely to occur only if the pore spaces in the snow were extremely large and the temperature

gradients very high, and concluded conditions sufficient for convection were unlikely in natural snow covers. Indeed, most recent models (e.g., Sommerfeld, 1983; Colbeck, 1983; Gulber, 1985; Christon et al, 1993; Satyawali et al, 1999) do not account for convective action.

Since vapor flux through the interstitial pore space is fundamental to kinetic-growth metamorphism, the snow must be sufficiently porous to facilitate significant mass transfer. Large faceted crystals tend to grow most readily in new snow or lightly compacted snow of low density where a large air space is present (Akitaya, 1974). In snow with densities greater than about 350 kg/m^3, the kinetic-growth process is inhibited and a "hard" depth hoar forms (Akitaya, 1974; Marbouty, 1980). The resulting crystals are still angular, but differ from normal depth hoar in that they are much smaller and possess considerable strength derived from a higher degree of bonding.

While an exact value for the critical temperature gradient necessary for kinetic-growth metamorphism is difficult to determine due to its dependence on temperature as well as snow density and structure (Adams and Brown, 1983; Colbeck, 1983), a vapor pressure gradient of 5 mb/m was found to be sufficient to initiate growth of faceted snow (Armstrong, 1985). Throughout the literature, a threshold temperature gradient between 10-20 deg C/m is typically cited.

A variety of conditions can exist within the snowpack that give rise to temperature gradients large enough to drive kinetic-growth metamorphism. The most common situation for permitting the growth of large faceted crystals occurs during early winter when the snowpack is shallow, air temperatures are cold, and the snow on the ground is

often of low density. These conditions are especially prevalent in continental, high-altitude climates where depth hoar is observed to grow nearly every season. Since the rate of metamorphism is an increasing function of temperature, the strongest faceting usually occurs near the ground at the base of the snowpack. Under these circumstances, the thermal gradient would be considered negative; that is, the temperature decreases in the direction of the snow surface causing a net upward transfer of water vapor. Field researchers (Perla and Martinelli, 1976) have also observed that faceted grains are often found above and below high-density crust layers formed from sun, rain, or wind action. This has been attributed to local increases in temperature gradient due to the higher thermal conductivity of the dense layer (Adams and Brown, 1983). Recently, more attention has been given to faceted snow that forms in the upper regions (top .20-.30 m) of the snowpack. These grains, which have been reported by many snow researchers and avalanche practitioners, are termed near-surface faceted crystals (Birkeland, 1998) and are typically much smaller than depth hoar. Birkeland (1998) identified three different sets of surface conditions which can give rise to very large temperature gradients in excess of 100 deg C/m.

In addition to altering the original crystal shape and size, kinetic-growth metamorphism significantly changes the thermo-mechanical properties of the snow. As the original snow crystals disappear during the recrystallization process, their bonds are also lost (Colbeck, 1983). Thus, bond formation cannot keep up with bond loss (de Quervain, 1963), and the bonds that do exist will be smaller relative to the new crystal. Furthermore, the majority of bonding that does occur takes place between grains that are

above or below each other, forming vertically-oriented chains of depth hoar crystals. While the snow maintains considerable compressive strength, shear strength rapidly decreases as kinetic-growth metamorphism progresses. The end result is a fragile "house of cards" scenario where the entire snowpack is weakly supported by depth hoar, often requiring only a small additional load to cause complete failure of the layer. As long as the snowpack remains cold, faceted grains are very resistant to rounding or bonding which would ultimately strengthen the snow. As a result, once faceted snow forms, it often remains a persistent threat in the mountain snowpack. Depth hoar resulting from kinetic-growth metamorphism is responsible for very large and destructive avalanches, often causing the entire snowpack to fail right down to the ground.

Kinetic-Growth Metamorphism Research

Kinetic-growth metamorphism has been the subject of more formal research than perhaps any other phenomena associated with the alpine snowpack. There has been a tremendous amount of investigative and experimental work done in both laboratory and field settings (i.e. de Quervain, 1963; Akitaya, 1967, 1974; Marbouty, 1980; Trabant and Benson 1972; Bradley et al,1977; Adams and Brown, 1982), in addition to theoretical studies attempting to model the complex physical processes involved with metamorphism (i.e. Colbeck, 1983; Adams and Brown, 1983; Christon et al, 1987; Gray and Morland, 1993). Early observations from field workers and snow practitioners identified depth hoar as a major cause of avalanches, thus underscoring the necessity of such research.

The conditions necessary for kinetic-growth metamorphism have been duplicated in the laboratory (de Quervain, 1963; Akitaya, 1967, 1974; Marbouty, 1980) and the resulting faceted crystals have been analyzed. The prevailing conditions in Fairbanks, Alaska, are very conducive to depth hoar formation, and detailed field observations, experiments, and analyses have been performed in this environment by Trabant and Benson (1972). Work has been done by Birkeland et al (1998) to measure the strong temperature gradients near the snow surface which often result in faceted snow occurring in the upper regions of the snowpack.

The result of previous research has been a thorough understanding of the physical processes that occur during kinetic-growth metamorphism. However, little work has been done to quantitatively describe the changes in snow microstructure (i.e. grain size, bond size, neck length, coordination number, etc.) during metamorphic processes. Consideration of snow microstructure has been shown to be important to accurately model kinetic-growth metamorphism, as well as other types of snow properties including viscosity and thermal conductivity (Brown, personal communication, 1999). The microstructural quantities used to describe the granular network of snow are numerous and diverse. Parameters that appear frequently in the literature include bond radius, neck length, number of bonds per grain, number of bonds per unit volume, volume of a single grain, intercept length, surface area per unit volume, and coordination number (Kry, 1975; Gubler, 1978; Perla, 1986; Hansen and Brown, 1986; Edens and Brown, 1994). The relative importance associated with each of these quantities seems to depend on the author and the formulation of the model that utilize them.

Despite the important role snow microstructure plays in metamorphic processes, very few laboratory investigations have attempted to measure the change in microstructural parameters of snow over time. In Switzerland, depth hoar was grown in a laboratory, and surface sections of samples taken from this depth hoar were analyzed in order to see how the snow microstructure changed with time (Brown, personal communication, 1999). A similar experiment was performed by Fierz and Baunach (2000), and while certain microstructural properties were measured, important parameters describing the nature of bonding between the snow grains were not taken into account.

Computed Tomography

A major impediment to research of this nature has been the destruction of the snow specimen that is being examined. Current techniques of snow sample analysis, whether looking at individual crystals under magnification or performing surface or thin sections,

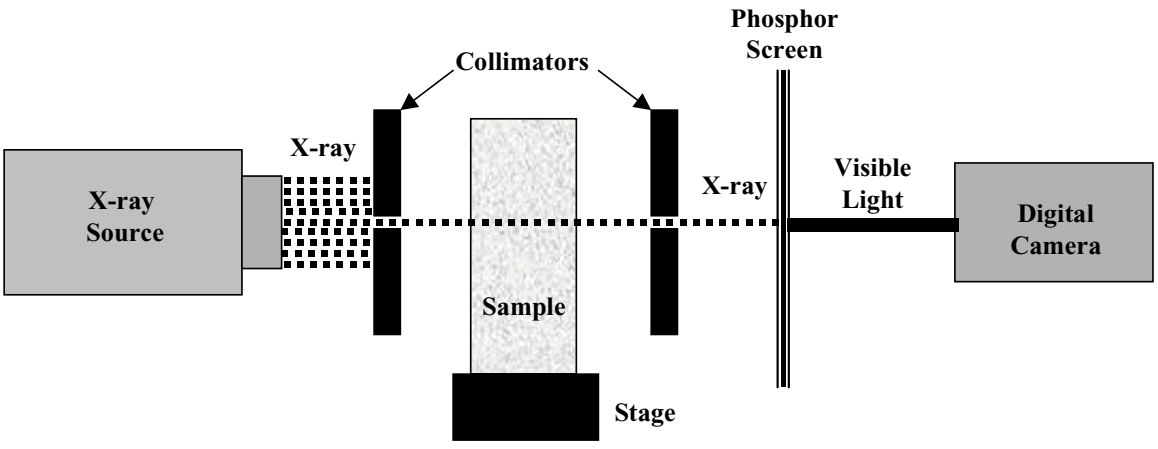

Figure 1. Illustration of CT scanner operation.

necessarily alter the specimen irreversibly. Up to this point, it has not been possible to continually analyze the properties of the *same* sample of snow during metamorphic processes. Many scientists have attempted to observe changes in snow properties over time by removing specimens of snow from a larger sample at regular intervals, but this introduces significant error due to spatial variation since each specimen is taken from a different location. Regarding recent metamorphism experiments, Brown reported significant scatter in their data because of this variability (personal communication, 1999). However, recent acquisition of CT scanners by several major research facilities worldwide have led to the development of a new tool for examining snow microstructure, one that allows nondestructive analysis of a snow sample.

Overview of Computed Tomography

Computed tomography (CT) uses an X-ray beam and digital camera to examine a cross-sectional slice of an object. The primary components of a CT scanner include an x-ray source, a sample stage, and a detection system (Figure 1). As the x-ray leaves its source, it travels through a collimator – two parallel lead plates – that narrow the beam into a flat, horizontal plane. This "plane" of x-ray transects the sample mounted to the stage and passes through another collimator before reaching the detector. The detection system consists of a phosphor screen that converts the x-ray into visible light and a high-resolution digital camera. The result is a very thin digital radiograph. This process is repeated, typically on one degree steps, as the sample or x-ray source is rotated through a full revolution. By taking many closely-spaced horizontal CT cross-sections along the

vertical axis of a sample, it is possible to reconstruct its three-dimensional internal structure.

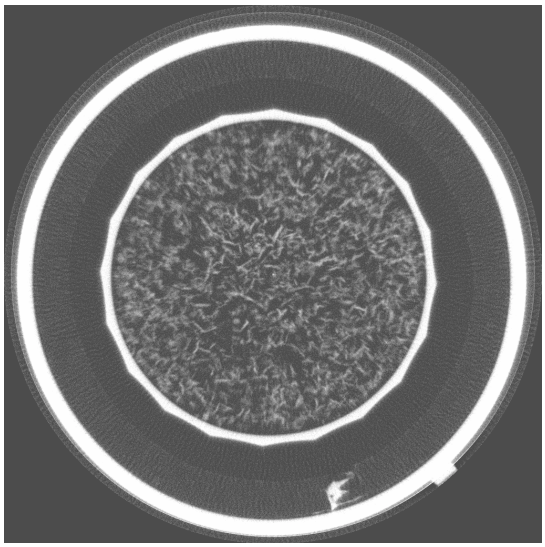

Figure 2. Two-dimensional CT image of faceted snow.

The variation in X-ray absorption of the sample is dependent on the density and, to a lesser extent, the chemical composition of the object, and it is represented by different intensities of light reaching the camera. By recording the plane of an object at many different angles through a full revolution, it is possible to mathematically extract the density of each point within the plane. This two-dimensional density map constitutes a CT image (Figure 2) and provides accurate information about the internal structure of an object. The utilization of computed tomography in the medical field is well known and its prevalence among other branches of science is increasing.

Application of Computed Tomography to Snow Research

Naturally, CT imaging is a promising tool to explore the internal structure of snow and ice. To date, its use in this regard is not well documented; however, several research institutions throughout the world have begun to explore its potential. The Swiss Institute for Snow and Avalanche Research (SLF) is currently in the process of acquiring a CT scanner (Lehning, 2000, personal communication), and in Japan, it has been used as a

tool for investigating the structure and three-dimensional density of sea ice (Kawamura, 1990). To date, the largest advances made in this area have been achieved by French researchers at the Centre d'Etudes de la Neige (CEN) (Coleou et al, 2000). Using computed tomography and a powerful reconstruction software, three-dimensional images with a resolution of 10 μm were obtained of a small snow specimen (9mm × 9mm cylinder). However, to achieve these results required over 200 hours of scanning for each sample, in addition to an unspecified amount of time for image reconstruction and analysis. At Montana State University, scientists have used a CT scanner to search for biological matter in Antarctic ice cores and to investigate deformation of snow under axial loads (Adams, personal communication, 1998), and have demonstrated the utility of CT technology to collect nondestructive, two-dimensional images of snow microstructure (Lundy and Adams, 1998).

Stereology

The characterization of snow microstructure has been neglected by the majority of laboratory studies; a likely reason is because it is exceedingly difficult to quantify. Not only are the microstructural features of snow challenging to measure accurately, the values of these parameters can vary widely within a single snow sample. In addition to a large number of measurements, statistics are needed to provide information regarding the variation of the microstructural parameters within the snow specimen.

Historical Background of Stereology

Stereology, which literally means "knowledge of space," is a term coined by Hans Elias in 1961 to describe the emerging branch of science that allowed observations made from thin cross-sections of a specimen to be interpreted in terms of the specimen's spatial structure. Weibel (1980) defined stereology as "A body of mathematical methods relating three-dimensional parameters defining structure to two-dimensional measurements obtained on sections of the structure." These techniques that yield three-dimensional information from two-dimensional observations are becoming prevalent in biology, geology, and material science. Stereological methods are statistical in nature and provide estimates of spatial structure.

In 1847, French geologist Auguste Delesse introduced the concept of determining volume density by measuring areal density of a random two-dimensional cross-section (Weibel, 1980). A. Rosiwal, another geologist, furthered this concept in 1898 when he computed the volume fraction of a certain constituent by measuring the fraction of a randomly drawn line that intersected the particular component. Stereological methods were introduced to biological research in 1943 by Harold Chalkney at the National Cancer Institute in Bethesda. Since then, these techniques have been used extensively to investigate the internal structure of organs from microscope slides and also to quantify various parameters of bacterial colonies. In general, the evolution of stereology tended to be pragmatic: as new applications posed unique problems, solutions were found that added to the body of stereological techniques (Weibel, 1980).

Application of Stereology to Snow Research

Kry (1975) was one of the first researchers to utilize stereological analysis in conjunction with surface sections to quantify micro-scale features of snow, in this case measurement of bonds was the primary focus. A similar study was conducted by Gubler (1978). More recently, the tedium associated with the measurement of such small-scale features has been reduced through the utilization of computers, which have become an essential tool in microstructural analysis. Perla et al (1986) used a computer program to compute stereological quantities from a digitized image of a serial section. In a more sophisticated formulation, Hansen and Brown (1986) developed a statistical model to characterize the granular structure of snow for use in a constitutive theory for high-rate deformation of snow. This statistical theory was used in conjunction with image analysis software and a digitized photo of a surface section, which allowed the authors to compute the stereological parameters needed to calculate the three-dimensional microstructural quantities. Even though the image analysis program aided in the measurement the stereological properties, much of the process was still done by hand.

Perhaps the most comprehensive stereological analysis software to date is a program developed by Edens and Brown (1994), which automatically computes microstructural measurements from a digitized image of a surface section. The most innovative step in the analysis is the "skeletonization" of the granular material. The process involves inscribing maximal disks (Figure 3a) into the network of snow grains, and the line segments which connect the centers of the disks become the skeleton (Figure 3b). Furthermore, each point along the skeleton is assigned a value given by the radius of the

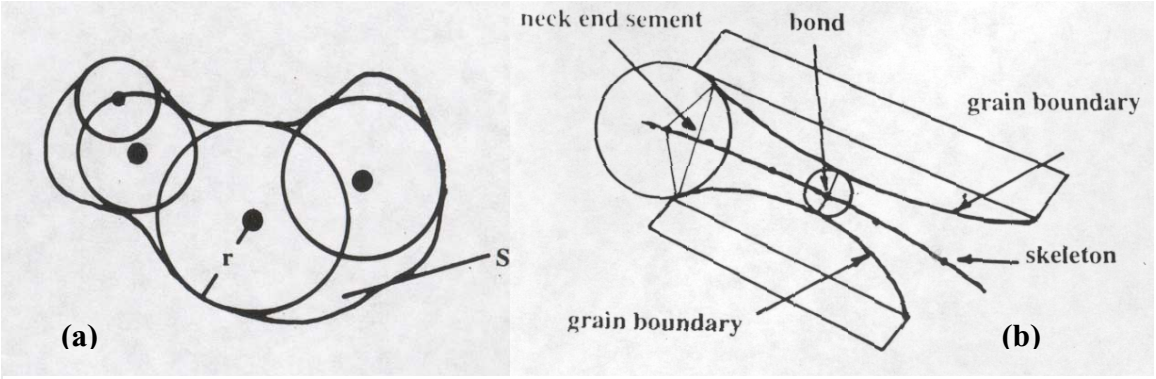

Figure 3. Skeletonization of the granular material. (a) Series of maximal disks incribed into a grain of snow. (b) Formation of the skeleton by connecting the centers of the disks.

maximal disk at that point. Skeletonization provides valuable information that can be used to define the curvature along the connected lattice of snow grains, and allows the identification of individual grains as well as the bonds and necks that link them. Bonds are located by defining a bond constriction ratio (Figure 4); a bond is identified if the ratio of radii of neighboring inscribed disks along the skeleton is less than a specified value. Once grains and bonds are identified, necks are modeled as truncated cones between the two. Edens' software then uses quantitative stereology to relate the two-dimensional measurements to the average three-dimensional properties of the sample. The major advantage of this program is that it

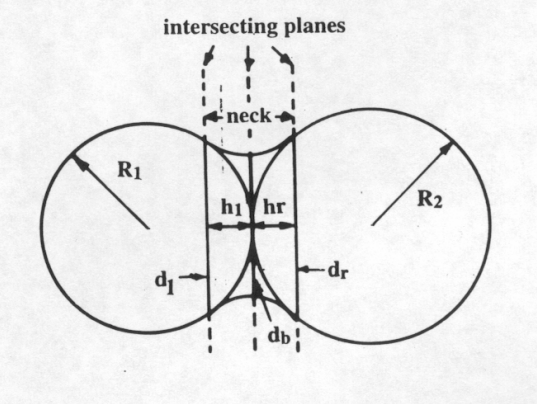

Figure 4. Geometry used by stereology software to define the bond and neck between neighboring snow grains.

is completely automated and repeatable – given the same digitized surface section, the analysis will yield identical results. When making stereological measurements by hand, this result is impossible to achieve. However, a limitation of the methodology is that it has not yet been developed to the point that anisotropic materials can be analyzed to determine three-dimensional microstructural properties.

Metamorphism Models

The bulk of the experimental work completed on snow metamorphism has been done not only to further the understanding of the processes, but also to augment efforts to model metamorphism using physical and mathematical theory.

Bader (1939) presented what might be considered the first model for kinetic-growth metamorphism of snow in his description of vapor flow between two parallel plates of ice with different temperatures. This approach utilizes the conservation of mass to calculate the one-dimensional diffusion of water vapor between the plates of ice. The model of Giddings and LaChapelle (1962) uses a similar approach, but make the assumption that all of the water vapor diffusing upward stops at the next level (Sommerfeld, 1983; Colbeck, 1987). Perla (1978) was one of the first researchers to recognize the granular nature of snow in his model (Colbeck, 1987), and incorporation of a more realistic geometry in order to better account for inter-particle effects would prove to be the crux of future metamorphism research. In the 1980s, a significant amount of metamorphism work began to include a simplified geometrical description of snow structure, and other

formulations introduced “shape” or “enhancement” factors to account for the variable snow microstructure. (i.e. Sommerfeld, 1983; Gubler, 1985; Adams and Brown, 1982; Adams and Brown, 1983; Colbeck, 1983),

Kinetic-growth metamorphism has also been modeled using modern mixture theories (Adams and Brown, 1989,1990; Brown et al, 1994), which describe the snow as a two-phase, granular material composed of ice and water vapor. Other researchers (i.e. Bader and Weilenmann, 1991; Gray and Morland, 1994) have used mixture theories to model snow as a four-constituent (three phases of water plus air), phase-changing continuum, but have not addressed the metamorphism of snow. While mixture theory allows a more detailed description of the interaction between the ice and vapor phases, the microstructure of the snow is still largely neglected. However, very recently a sophisticated theory was developed by Brown et al (1999) that uses both mixture theory as well as a description of snow microstructure to model equilibrium metamorphism. An important aspect of this model, and one that will play a large role in its validation, is that the microstructural properties (grain size, bond size, neck length) it incorporates can be measured in actual snow using the stereological techniques described in the previous section. This mixture theory of snow represents the cutting edge of current metamorphism theory, but at the present time is not applicable to kinetic-growth metamorphism.

Although the metamorphism theory of Satyawali et al (1999) does not use mixture theory, it is the only kinetic-growth metamorphism model that incorporates microstructural properties such as grain size, bond size, neck length, and mean pore

length. By assuming a simple body-centered cubic arrangement of snow grains, the temperature gradient both in the pore space and across the bonds between grains is calculated, and the associated diffusion of water vapor is determined. Changes in the microstructural properties of the snow due to the transference of water mass are then found.

It has become well-acknowledged that the consideration of snowpack microstructure is a necessary requisite to accurately modeling the behavior of snow, especially the metamorphic processes. Addressing the small-scale properties of snow provides a means for directly comparing the model results to measurements, which is paramount to the validation of theory. The success of future work will depend largely on advancements made in relating properties calculated by models to those measured in actual snow, a problem for which stereology may provide a solution.

In addition to physically-based models, another approach has been used to simulate kinetic-growth metamorphism based on experimental data. From results obtained in laboratory-based metamorphism experiments, Marbouty (1980) formulated an empirical equation to predict changes in density and grain size in snow undergoing kinetic-growth metamorphism. This grain-growth equation was later incorporated into CROCUS, a French snow cover model (Brun et al, 1992).

Modeling the Evolution of the Mountain Snowpack

Recent advances in snow research, as well as the increasing availability of powerful computer systems, have led to the development of several computer models that are able to predict the evolution of a mountain snowpack with varying degrees of accuracy. Most of these programs use common meteorological parameters as inputs, either measured directly at mountain weather sites or inferred from meteorological and atmospheric models, and provide as output predicted snowpack temperature, density, and in some cases, grain size and texture. The more advanced models have already been used operationally and provide avalanche hazard forecasters and other mountain safety experts with yet another tool for evaluating the alpine snowpack.

Morland et al (1990) introduced a theory that modeled the snowpack as a continuum mixture of ice, liquid water, water vapor, and air. The resulting system of partial differential equations was sufficiently complex to require a number of simplifying assumptions before any numerical solutions could be performed. Bader and Weilenmann (1992) reduced the general theory to a one-dimensional model they called DAISY, and using simplified initial and boundary conditions, arrived at solutions using numerical techniques. The mixture theory was also simplified and solved numerically by Gray and Morland (1994), who assumed a one-dimensional, two-phase system consisting only of ice and dry air. While allowing for phase change and the calculation of density and temperature profiles of a theoretical snow cover, the limitations of these early models lie mainly in their neglect of snow microstructure. Without even elementary microstructural

quantities such as grain or bond size, metamorphism of the snow is not predicted and many of the constitutive properties of snow cannot be formulated accurately. However, the theoretical basis and absence of empiricism in these theories laid a solid foundation for more sophisticated models.

Since these early snowpack models were solved only for simplified boundary conditions and theoretical snow covers, their practical value was limited. No provisions were made to utilize meteorological measurements from the field as inputs to the model. Additionally, with the exception of temperature and density, several key snowpack properties were not predicted.

A more sophisticated model called SNTHERM (Jordon, 1991) was developed by the Cold Regions Research and Engineering Laboratory (CRREL), primarily to predict temperatures within the snowpack and especially at the snow surface. The model calculates a numerical solution for a snow cover with variable layering, and uses data from meteorological instruments as surface boundary conditions. Even though SNTHERM takes a significant step forward in modeling a realistic snowpack with measurable boundary conditions, it contains only rudimentary provisions for snow metamorphism and therefore does not make useful predictions regarding snowpack layering and structure.

Operational use of a snow cover model began with a French model named CROCUS (Brun et al,1989), which has been used as a tool for the country's avalanche forecasters since 1988. CROCUS began as an energy and mass model, predicting the settlement, phase change, and the density and temperature profiles within the snowpack. Later,

empirical metamorphism laws were introduced to allow CROCUS to simulate changes in grain size and shape, giving the model the capability to predict the actual stratigraphy of the snow cover (Brun et al, 1992). While the formulations governing energy and mass transfer in CROCUS are largely based on physical principles, other aspects of the program, including viscosity, thermal conductivity, and changes in grain size and type, are controlled by empirical relations. While substantial, if not exhaustive, experimental work was completed in order to arrive at these equations, empirical relations by necessity simplify complex interactions and therefore often limit the amount of accuracy that can be achieved.

Recently, significant advances in the utility of the model have been made by incorporating CROCUS with a large-scale meteorological model (SAFRAN) and an expert system that estimates the snowpack stability (MEPRA) (Durand et al, 1999). Together, these components form an integrated, regional system that simulates meteorological parameters, snowpack characteristics, and avalanche hazard for a variety of spatial and elevational zones.

Perhaps the most sophisticated of the snow cover evolution models, and the focus of this thesis, is a program developed by the Swiss Institute for Snow and Avalanche Research called SNOWPACK. SNOWPACK is a predictive model that uses Lagranian finite elements to solve for heat and mass transfer, stresses, and strains within the snowpack (Lehning et al, 1998). Snow is modeled as a three-phase porous media consisting of volumetric fractions of ice, water, and air. The model contains both equilibrium and kinetic-growth metamorphism routines that calculate the time rate of

change of grain shape parameters sphericity and dendricity, grain radius, and bond radius which define the microstructural characteristics of the snow. Other variables such as coordination number and bond neck length are computed from these primary quantities. Phase change of the ice and water components is taken into account, and a simple procedure for meltwater percolation through the snowpack is also utilized. Importantly, the conservation laws for mass, energy, and momentum are adhered to in all aspects of the code. Currently, wet snow metamorphism is still under development, and the models for dry snow metamorphism are being improved (Lehning et al, 1998).

The SNOWPACK model uses the somewhat unfamiliar crystal type descriptions dendricity and sphericity introduced by Brun et al (1992). Dendricity can vary from 0 to 1 and describes how much of the original precipitation crystal form is still present in the snow. Sphericity ranges from 0 for completely faceted grains to 1 for rounded particles. Figure 5 relates dendricity and sphericity to the international snow classification symbols. New snow, for example, is assigned a dendricity of 1 and a sphericity of .5.

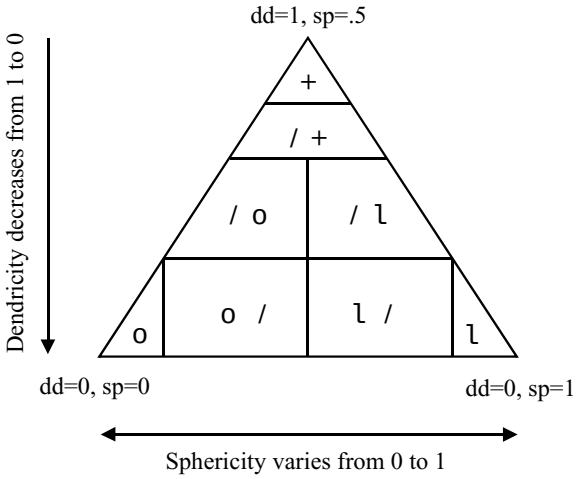

Figure 5. Relation of the model parameters sphericity and dendricity to the ISCI symbols.

The snow viscosity, η, of the snowpack is governed by a constitutive relationship based on that developed by Mahajan and Brown (1993), and accounts for complicated

processes including pressure sintering and surface tension effects. The constitutive theory yields the following proportional relations (Lehning et al, 1998):

$$\eta \sim \left(\frac{r_b}{r_g}\right)^6, \quad \eta \sim \left(\frac{N_3}{l}\right), \quad \text{and} \quad \eta \sim \theta_i^3, \tag{1}$$

where r_b and r_g are the bond and grain radii, N_3 is the three-dimensional coordination number, l is the bond neck length, and θ_i is the volumetric fraction of ice. An accurate modeling of the snowpack settling rate is especially important to SNOWPACK as it is used indirectly to estimate new snowfall. The snow depth measured at the weather station is compared to the modeled depth and the difference is taken as new snow, but only if certain conditions such as high relative humidity and low shortwave radiation are present. If the model determines that new snowfall occurred, additional elements are added to the top of the snowpack. New snow is automatically given an initial dendricity equal to 1, sphericity of .5, grain size of 0.6 mm, and density estimated from an empirical formulation dependent on air temperature, snow surface temperature, relative humidity, and wind speed (Lehning et al, 2000a). Estimation of the new snow density is critical to maintaining an accurate mass balance in the snowpack.

Calculation of the temperature profile in the snow cover is crucial as this parameter is key to accurate prediction of snow metamorphism. SNOWPACK has provisions for using several different thermal conductivity models, but the preferred theory is one adapted from Adams and Sato (1993).

Snow metamorphism and associated changes in the microstructure are calculated by the model using two separate theories: the first applies to low temperature gradients (<10

deg C/m) and predicts equilibrium metamorphism (Brown et al, 1999), the second is for larger temperature gradients that cause kinetic-growth metamorphism (Satyawali et al, 1999). Development of the grain shape parameters sphericity and dendricity resulting from the metamorphic processes are calculated from empirical equations following those from Brun et al (1992). An important aspect of the formulation of the theories used by SNOWPACK is the majority of them are physical models based on snow microstructure, which means they need adjustment than empirical models and are more widely applicable to different geographic locations and climates.

Reflected rather than incident solar radiation is used as an input to SNOWPACK since it allows the measurement instrument to be pointed downward, preventing it from becoming covered by snowfall or rime. To determine the incoming shortwave radiation, SNOWPACK uses a model for the snow surface albedo, either one based on meteorological parameters or characteristics of the snow at the snowpack surface (Lehning et al, 2000a). Both relations are empirical and based on three years of measurements. The amount and depth of short wave radiation penetration is governed by an exponential extinction function, with a coefficient that varies linearly with density (Lehning et al, 2000a).

Required as inputs to SNOWPACK are data normally collected from a remote alpine weather station, in addition to a few more specialized measurements. These include air temperature and relative humidity, total snow depth, wind speed, reflected shortwave radiation, snow surface temperature, and snowpack temperatures at specific depths. The model uses these data as boundary conditions to solve the equations that describe the

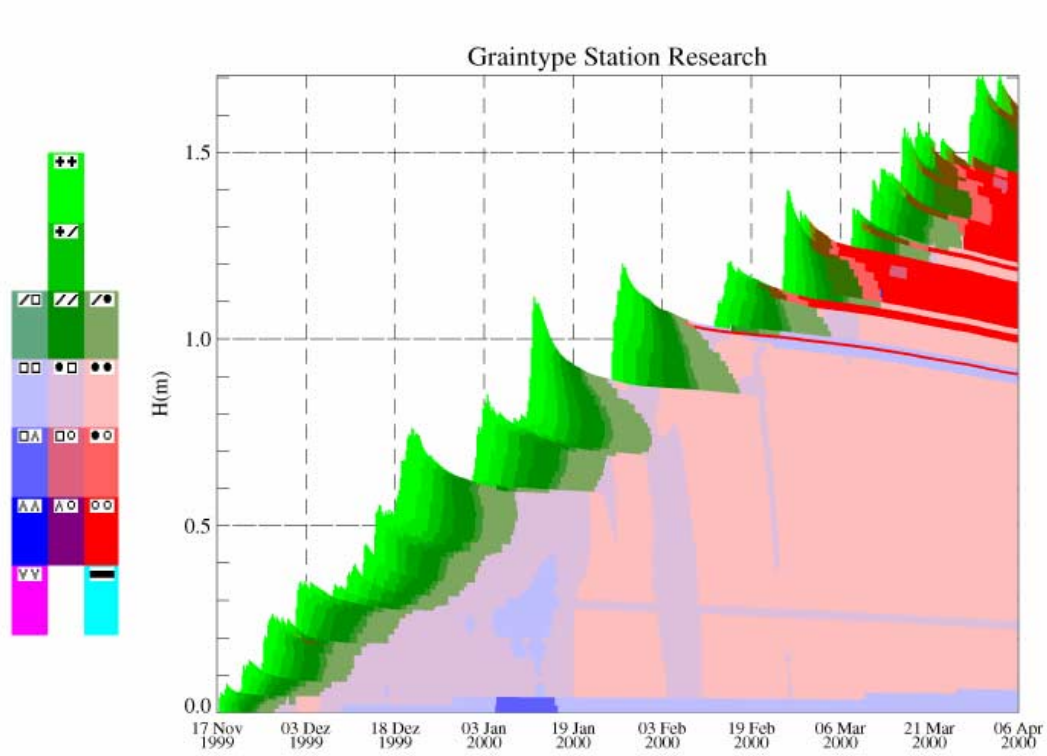

Figure 6. Sample GUI output of the SNOWPACK model.

character of the snowpack. The output of SNOWPACK is processed through a graphical user interface (GUI) that provides a convenient visual representation of the predicted snowpack. The typical output format is demonstrated in Figure 6; time is given on the horizontal axis, snow depth on the vertical axis, and the parameter of interest is plotted on a color scale. This provides an effective visualization of both the temporal and spatial distribution of the modeled variables, and allows the evolution of snow layering and the settlement of the snow cover to be observed. Such plots are available for the majority of the parameters calculated by snowpack, including density, grain size, bond size, temperature, temperature gradient, among others. In addition, SNOWPACK has the capability to output raw numeric data if so required.

One problem associated with the efforts to model the evolution of a mountain snowpack is the lack of a meaningful comparison between the prediction of a model and the actual snowpack. Plots of simulated and measured snowpack parameters are abundant in the literature, but simply comparing these graphs visually does not provide a useful or consistent evaluation of the similarity between observed and predicted values. Introducing statistical methods into these comparisons would provide a means whereby the accuracy of the models could be quantified using well-established measures.

CHAPTER 2

PURPOSE

Field Investigation

Over the past decade, numerical models have been developed that simulate some or all of the complex processes occurring within the mountain snowpack. The level of sophistication of these models has increased to the point where a few of them, most notably SNOWPACK and CROCUS, have been in use operationally for the past several years. To date, the validation of the snowpack simulation models has been a weak point in the work associated with these models, one that will continue to limit their effectiveness and acceptance. Very few independent users are willing to expend the resources necessary to operationalize a snowpack model without first having access to an extensive evaluation of the program.

To complete the comparison, a weather station was constructed to provide the meteorological parameters necessary to run SNOWPACK, and regular snow profiles were conducted to provide a benchmark for the model output. Over the course of the 1999-2000 winter, the meteorological data was input into SNOWPACK, and a "predicted" snowpack was computed by the model. Finally, the use of statistical methods allow a thorough and objective comparison of the model output to data gathered during the field studies.

Laboratory Investigation

The primary objective of the laboratory component was to develop a method for obtaining detailed measurements of microstructural changes over time in snow undergoing kinetic-growth metamorphism. An additional goal was to test the technique by conducting actual experiments and acquiring a preliminary data set. Since the more advanced metamorphism models (i.e. Brown et al, 1999; Satyawali et al, 1999) now account for snow microstructure, accurate experimental measurements of the small-scale properties of snow will aide in improving the existing models and in the development of new theories.

While snow subjected to a large temperature gradient has been the subject of numerous laboratory investigations dating back to Akitaya (1974), never before has this concept utilized such sophisticated technology. The application of CT imaging to this research allows the same snow specimen to be sampled repeatedly throughout the course of the experiment. This innovative technique eliminates errors due to spatial variation that have plagued previous work, and provides a means to collect numerous cross-sectional images of the snow sample in a short period of time. Additionally, the digital images produced by the CT scanner are well-suited to analysis by an automated stereology software (Edens and Brown, 1994) which allows microstructural properties to be measured consistently and accurately. The utilization of these technological advances

greatly simplifies the data collection process, while simultaneously allowing more accurate measurements, resulting in higher sampling frequency and a more complete data set.

CHAPTER 3

METHODOLOGY

Field Investigation

Description of Field Site

Location. The field research site is located approximately one kilometer north of the Bridger Bowl Ski Area near Bozeman, Montana, in an area known as Wolverine Basin.

Figure 7. Aerial photo showing location of Wolverine Basin weather station.

This region falls within the intermountain or transition climate regime as defined by McClung and Schaerer (1993). An average annual snowfall of approximately 900 cm is measured at the adjacent ski area. The site is a large, open, relatively flat meadow (approximately 100 m by 75m) situated at an elevation of 2240 m (Figure 7).

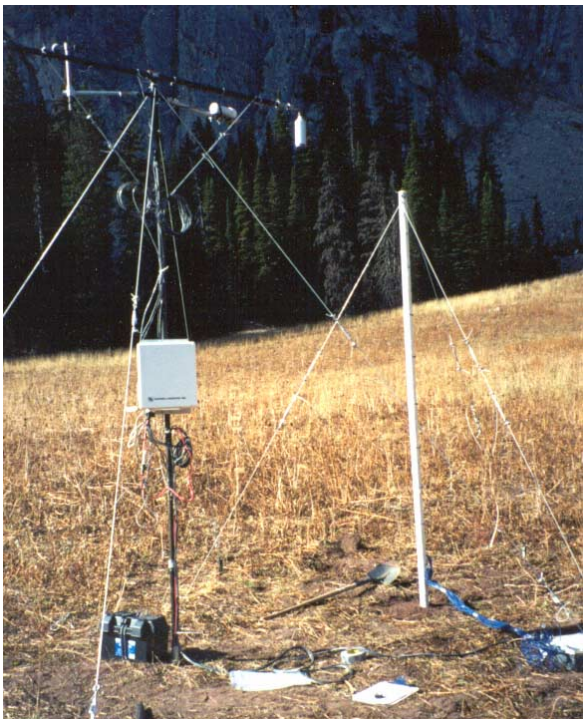

Figure 8. Wolverine Basin weather station.

Instrumentation. Comprising the site is an instrument tower and temperature-measurement array (Figure 8). The tower is

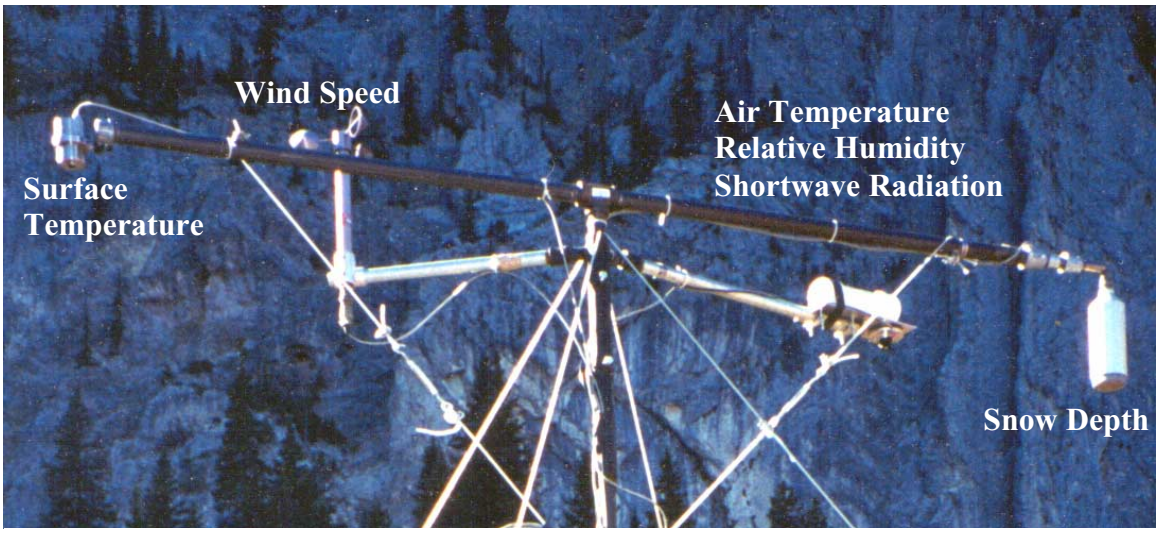

Figure 9. View of instruments mounted on weather station tower.

3.5 m tall and constructed from 38 mm steel pipe. There are two booms at the top that form a "T" configuration (Figure 9); on the ends of these are mounted the snow depth and snow surface temperature sensors. The tower-mounted instruments are summarized in Table 1, and are logged by a Campbell Scientific CR10X powered by a 12 V lead-acid battery and MSX10R Solar Panel.

Parameter	**Instrument**
Air Temperature	Campbell Scientific 107 Temperature Probe
Relative Humidity	Campbell Scientific 207 Relative Humidity Probe
Snow Surface Temperature	Everest Interscience 4000.4ZL Infrared Thermometer
Snow Depth	Cambpell Scientific UDG01 Ultrasonic Depth Gauge
Reflected Solar Radiation	Li-Cor LI-200SA Pyranometer (400-1100 nm)
Wind Speed	Met-One 014A Anemometer

Table 1. Description of weather station instruments.

The temperature-measurement array was utilized to obtain a detailed, real-time temperature profile within the snowpack. It is constructed from a 3 m PVC tube fitted with Type T thermocouples on 5 cm intervals, which stands vertically with the bottom thermocouple at ground level. The PVC tube is filled with foam so that the entire unit has a low thermal conductivity. The resulting 60 channels of temperature data are wired into two Campbell Scientific AM416 32-channel multiplexers which are housed in a separate enclosure located near the bottom of the array. In addition to providing temperatures at the 25, 50, and 100 cm levels as required by the Swiss model, it provides a complete temperature profile of the snowpack, and when combined with data from the snow depth

gauge and snow surface temperature, this arrangement provides adequate resolution for investigating near-surface temperature gradients.

The datalogger runs a program that samples the instruments every minute, and outputs the averages on a 15 minute basis. An exception occurs with the snow depth gauge, which requires some error-checking algorithms prior to output. On a weekly basis, a Campbell Scientific SM192 Storage Module is brought to the site and the datalogger memory is downloaded.

Data Collection Procedure

The field site was visited weekly for data collection (Figure 10). At this time, the data is downloaded from the remote datalogger and a snowpit profile is conducted. The snowpits are excavated in undisturbed, fenced-off snow near the instrument tower.

Figure 10. Weekly collection of snowpack observations.

Density is measured with a triangular density box of known volume, and weighed on a portable digital scale. Grain diameter and the ISCI classification (Colbeck et al, 1990) were determined with a 30× Pentax hand lens. Snow strength was estimated with a hand hardness test (McClung and Schaerer, 1993). Observations were recorded every 10 cm

through the full depth of the snowpack. In addition to these standard measurements, depth and thickness of notable layers such as melt-freeze or wind crusts was noted.

Prediction of the Snow Cover Evolution with SNOWPACK

A complete meteorological data set was obtained from November 17, 1999 to April 6, 2000, which includes the following parameters measured on 15 min intervals: air temperature, snow surface temperature, relative humidity, reflected shortwave radiation, snow depth, wind speed, and snowpack temperatures measured at 25, 50, and 100 cm above the ground. Using a spreadsheet, the data was arranged in a tabular text file and then used as input to the SNOWPACK model. The model itself was configured to output the snow profile data for each day at 1100 hours, which corresponded with the time at which the snowpits were typically performed in the field. It is this profile data that is compared to the weekly snowpit observations.

Comparison of the Predicted Snowpack to the Observed Snowpack

While SNOWPACK includes a graphical user interface that presents a visual description of the snowpack predicted by the model, a simple visual comparison of the model results to the snowpit data is not adequate to conclusively rate the capabilities of the model. Certain features of the snowpack, such as melt-freeze crusts and other specific layers, certainly benefit from a visual comparison to the graphical model output, but other properties that are more numeric in nature (i.e. temperature, temperature gradient, density, grain size, and grain type) are better evaluated through statistical methods.

Mapping and Interpolation of the Simulated Snowpack Data. Before any comparison of the numeric data can be undertaken, predicted model data must be calculated at the same depths within the snowpack as the snowpit observations. To accomplish this task, a technique was devised by Lehning et al (2000b) to obtain model results at desired locations.

First, the difference in modeled and observed total snowpack height must be taken into account. Any error in the predicted settling rate will shift the layering of the snowpack up or down. While it is probable that certain regions of the predicted snowpack are more likely to have settling rate errors, it is more practical to perform a linear mapping of the modeled data so that all heights are adjusted in proportion to the distance from the ground. Let $z_k^{'\mathrm{mod}}$ describe the heights of the data output by the model, where n is the number of levels and k is an index and ranges $0 < k < n$. Additionally, define $z_n^{'\mathrm{mod}}$ and z_n^{obs} as the modeled and observed total snow depths. Then the new mapped heights, z_k^{mod}, are given by

$$z_k^{\mathrm{mod}} = z_k^{'\mathrm{mod}} \frac{z_n^{obs}}{z_n^{'\mathrm{mod}}} . \qquad (2)$$

The end result of the mapping is that the modeled and observed snowpacks now have the same height and the model data heights are adjusted accordingly.

Since density is a volumetric property, it will need to be adjusted according to the new mapping. For each mapped height z_k^{mod}, an adjusted density ρ_k^{mod} is calculated. If $\rho_k^{'\text{mod}}$ is the original density, then

$$\rho_k^{\text{mod}} = \rho_k^{'\text{mod}} \frac{z_k^{'\text{mod}} - z_{k-1}^{'\text{mod}}}{z_k^{\text{mod}} - z_{k-1}^{\text{mod}}} . \quad (3)$$

Temperature gradients were computed by taking the mean of the forward-calculated and back-calculated temperature gradient:

$$\frac{dT_i}{dz} = \frac{\left(\frac{T_{i-1} - T_i}{z_{i-1} - z_i}\right) + \left(\frac{T_i - T_{i+1}}{z_i - z_{i+1}}\right)}{2}, \quad (4)$$

where T_i and z_i are the respective temperature and depth coordinate at height i. This equation is applied directly to the measured temperatures on 10 cm intervals. For the modeled temperatures, the temperature gradients are calculated prior to the linear mapping of the predicted snowpack in order to preserve the original temperature spacing.

After the mapping is completed, we can linearly interpolate between mapped heights to obtain model results at the desired locations within the snowpack; in other words, at heights that coincide with the observed measurements. This method is appropriate for point measurements such as temperature, temperature gradient, and grain size, but will also be applied to density, even though it is in fact a bulk measurement. For a series of observations such as temperature T_i^{obs}, at snow depths z_i^{obs}, a linear interpolation between the two neighboring model heights, z_k^{mod} and z_{k-1}^{mod} ($z_{k-1}^{\text{mod}} < z_i^{obs} < z_k^{\text{mod}}$), yields a modeled temperature at the observed height:

$$T_i^{mod}(z_i^{obs}) = \frac{z_k^{mod} - z_i^{obs}}{z_k^{mod} - z_{k-1}^{mod}} T_k^{mod} + \frac{z_i^{obs} - z_{k-1}^{mod}}{z_k^{mod} - z_{k-1}^{mod}} T_{k-1}^{mod} . \quad (5)$$

In this case, m is the number of observations levels and i is an index that varies from $0 < i < m$.

The equations for calculating temperature gradient, grain size, bond size, and density are identical. Since grain type is not measured on a continuous numeric scale, interpolation is not applicable. No realistic assumptions can be made regarding the behavior of grain type between mapped heights, so the only feasible technique is then to use the grain type value that occurs at the height closest to the observed location.

This methodology is much simplified by having collected snowpit data as point measurements taken on a regular height interval. However, many observers collect snowpack information in a different format, focusing on the layering and measuring snow properties for thicker layers of homogenous snow, since it is quicker and more useful for evaluating avalanche hazard. In this situation, additional calculations are required to compare regions of interest found in the model and in observations (Lehning et al, 2000b).

The preceding algorithms were programmed into a C code that inputs the SNOWPACK output files as well as a text file containing formatted snowpit observations. After the calculations are completed, the program creates an output file containing the observed and modeled data at the same heights within the snowpack. This file was in turn opened in a spreadsheet where the data was manipulated and the statistical analyses were performed.

Grain size is inherently a subjective measurement; snow grains often have different diameters depending on which axis it is measured. Snow observers often measure the largest diameter of a snow crystal, and therefore tend to overestimate the grain size. Alternatively, SNOWPACK defines grain size as the diameter of the largest sphere that can be completely contained within the snow grain. Because of this discrepancy, a normalized grain size will be computed and analyzed in addition to the original grain size. The modeled and observed grain sizes, rg_i^{mod} and rg_i^{obs}, are normalized according to the smallest and largest grains in each profile:

$$rg_i^{norm} = \frac{rg_i - min(rg)}{max(rg) - min(rg)} \tag{6}$$

Note that this normalization is done independently for both the predicted and observed data. The result is a normalized value for the grain size that lies between zero and one.

Statistical Comparison of Numeric Data. For temperature, temperature gradient, density, and grain size, a variety of statistical measures were utilized to gain a complete evaluation of the SNOWPACK model's ability to simulate these variables.

In order to determine the degree of correlation between the modeled and observed values, the Pearson's correlation coefficient was computed. Pearson's r is found in the following manner (Box et al, 1978):

$$r = \frac{\sum_{i=1}^{n} x_i^{mod}\, x_i^{obs}}{\sqrt{\sum_{i=1}^{n} (x_i^{mod})^2 \sum_{i=1}^{n} (x_i^{obs})^2}}, \tag{7}$$

where x_i^{mod} and x_i^{obs} are a set of n predicted and measured parameters. Pearson's correlation coefficient is a measure of the degree of linear relationship that exists between a set of paired data. A perfect positive correlation ($r = 1$) exists if every time x_i^{mod} increases, x_i^{obs} goes up by the same proportion. On the other hand, a perfect negative correlation ($r = -1$) exists if every time x_i^{mod} increases, x_i^{obs} decreases by a constant proportion. The correlation test provides insight into whether SNOWPACK is correctly simulating the trends of a specific variable, but does not take into account the absolute accuracy of the data.

In order to ascertain the difference between the modeled and observed quantities, a simple mean square error analysis was also performed. The mean square error (MSE) given by (Box et al, 1978):

$$MSE = \sqrt{\frac{\sum_{i=1}^{n} (x_i^{mod} - x_i^{obs})^2}{n}}. \qquad (8)$$

The final analysis will be a linear regression of the simulated data on the observed data, which fits a straight line to a set of independent and dependent data points based on a least-squares fit (Box et al, 1978). In this case, linear regression answers the following question: given x_i^{mod}, can an equation of the form

$$x_i^{obs} = b_1 x_i^{mod} + b_0 \qquad (9)$$

be found to accurately predict x_i^{obs}? For the purpose of this analysis, the linear regression will be utilized as a tool to examine the relationship that exists between the predicted and

measured data. If x_i^{mod} is equal to x_i^{obs}, one would expect the intercept b_0 to be close to zero, and the slope b_1 should be nearly one. Additionally, the multiple correlation coefficient R^2 associated with the regression will indicate how well the data falls along the line.

Comparison of Grain Type. Comparison of predicted and observed grain type poses a problem as it is not measured on a continuous numeric scale, and therefore does not lend itself to the procedures presented above. To resolve this issue, an alternate method will be used combining a *Chi-square* (X^2) statistical test with a proprietary technique adapted from Lehning et al (2000). While this methodology is not as robust as that used for the numerical parameters, it still provides meaningful results.

The X^2 is a non-parametric statistical measure that can be used to ascertain the degree of similarity between two populations that are categorical in nature. For a complete description of the test, see Siegel and Castellan (1988). As a means of gauging the X^2 value, Cramer's *phi* is calculated, which is given by

$$\Phi = \sqrt{\frac{\mathrm{X}^2}{N(a-1)}}, \tag{10}$$

where N is the number of samples in the population, and a is the number of categories present in the two populations, whichever is smaller. In this case, there are seven different grain classifications, so $a = 7$. Computation of Cramer's Φ is convenient as it can be interpreted in the same fashion as Pearson's *r*. The test is completed twice; once for the majority grain type $F1$, and again for the minority classification $F2$.

In addition to the statistical test, an original procedure is utilized that ranks the "closeness" of a data set containing modeled and observed grain types (Lehning et al, 2000b). Each modeled and observed height in the snowpack is characterized by a majority grain type $F1$ and a minority grain type $F2$. Then a distance measure d_k^{ij} is assigned for each combination of $F1$ and $F2$:

$$d_k^{11} = F1_k^{\text{mod}} \otimes F1_k^{obs} \;,\; d_k^{22} = F2_k^{\text{mod}} \otimes F2_k^{obs}$$

and (11)

$$d_k^{12} = F1_k^{\text{mod}} \otimes F2_k^{obs} \;,\; d_k^{21} = F2_k^{\text{mod}} \otimes F1_k^{obs}$$

Recall that k indexes the height level within the snowpack and ranges $0 < k < n$. The operator $\otimes$ is defined by a comparison matrix (see Table 2), and assigns a somewhat arbitrary value to the given combination of modeled and observed grain types that ranks their "closeness".

$F_k^{mod} \otimes F_k^{obs}$			MODEL	INTL	1	2	3		4		5		6		7
				SLF	1	2	3		4		5		7		6
					+	/	l		¤		Λ		¡		V
OBS				E			< 0.5	> 0.5	< 0.5	> 0.5	< 1	> 1	< 0.5	> 0.5	
INTL	SLF		E	i	1	2	3	4	5	6	7	8	9	10	11
1	1	+		1	0	0.2	0.3	0.4	0.8	0.9	1	1	0.5	0.5	0.5
2	2	/		2		0	0.2	0.3	0.6	0.7	0.9	1	0.5	0.5	0.5
3	3	l	< 0.5	3			0	0.1	0.6	0.8	0.8	0.9	0.5	0.5	0.5
			> 0.5	4				0	0.7	0.9	0.6	0.8	0.5	0.5	0.5
4	4	¤	< 0.5	5					0	0.1	0.3	.4	0.5	0.5	0.5
			> 0.5	6						0	0.1	0.2	0.5	0.5	0.5
5	5	Λ	< 1	7							0	0.1	0.5	0.5	0.5
			> 1	8								0	0.5	0.5	0.5
6	7	¡	< 0.5	9									0	0.1	0.5
			> 0.5	10										0	0.5
7	6	V		11											0

Table 2. Matrix defining the numerical distance measure of a particular modeled grain type from an observed grain type.

Defining further,

$$d_k^{straight} = \frac{d_k^{11} + d_k^{22}}{2}$$

and (12)

$$d_k^{cross} = \min\left(1, 0.1 + \frac{d_k^{12} + d_k^{21}}{2}\right)$$

where 0.1 is added to the cross term to account for the majority-minority mismatch. From the two quantities in (12), a measure of agreement for the crystal types at height k can be found:

$$d_k^{type} = \min\left(d_k^{straight}, d_k^{cross}\right). \quad (13)$$

The distance measure d_k^{type} varies from 0 when there is complete agreement between the simulated and observed grain types for the given height level *k*, to 1 when there is no similarity among the grain classifications for the level. Since the predicted and observed data occur on an even interval, no weighting is necessary and a final value can be computed as the average of all d_k^{type}'s:

$$d^{type} = \frac{\sum_{k=1}^{n} d_k^{type}}{n}. \quad (14)$$

Laboratory Investigation

Experiment Configuration and Procedures

Specimens of natural snow were subjected to large (50-65 deg C/m) temperature gradients in a controlled, laboratory setting. In order to facilitate the removal of the snow samples from the experiment configuration, the specimens were contained in three plastic drinking cups. One sample was used for temperature measurement, another is reserved for CT scanning, and the last is a backup. The cup is 148 mm tall, with an upper diameter of 72 mm tapering to a bottom diameter of 53 mm (Figure 11). The cup is vertically tapered to ensure that as the snow settles, it maintains contact with the sides of the cup. If the cup had vertical walls, the snow would pull away from the sides, leaving air gaps that would affect the heat and vapor transfer. Plastic wrap was placed on the top of the samples to eliminate any loss of mass through sublimation. The three sample cups were then inserted into an insulating foam block that is 46 cm square (Figure 12). The foam block and cups rest on an artificial "ground" which is an aluminum plate that is maintained at a constant temperature (Figure 13). The temperature variation across this plate was measured to be less than one degree.

Figure 11. Snow contained in tapered sample cup and covered with plastic wrap to prevent mass loss.

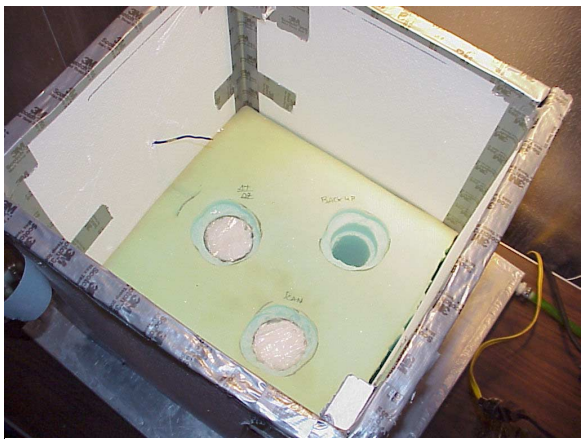

Figure 12. Snow samples in insulating foam block. Also visible is the thermocouple wire for measuring ambient temperature.

Figure 13. Experiment configuration showing styrofoam box, aluminum temperature plate, and heating system.

The entire apparatus is enclosed in a styrofoam box that adds thermal mass to the system and minimizes any influence of the air circulation within the cold room caused by the refrigeration fans.

Temperatures within the experiment were monitored daily on six thermocouples. One was mounted directly on the aluminum plate and another measured the ambient air temperature within the styrofoam box (visible in Figure 12). The remaining four were attached to one of the sample cups at regular intervals along the vertical axis in order to measure the temperature profile within the snow specimen.

Description of Snow Used for Samples

The experiment was run three times with snow of differing type and density, and once with ice spheres of uniform diameter. The snow for the tests was collected from mountain locations and transported to the cold lab in a cooler. For each experiment, the

average grain size and predominant crystal type were determined with a hand lens. For the first two experiments, the sample cups were filled by scooping the snow by hand and pouring it into the cups, then cutting the snow flush with a knife. In order to achieve a more uniform specimen, the cups were filled by sieving snow through a 4 mm sieve for Experiment 4. The average density of the snow sample was measured by weighing a sample cup filled with snow and measuring the volume of the cup. Characteristics of the snow used in each experiment are summarized in Table 3.

Experiment	**Crystal Type (ISCI)**	**Grain Size (mm)**	**Density (kg/m^3)**	**Mean *dT/dz* (deg C/m)**
1	/	0.5 - 1	230	60
2	/	0.5	130	55
3	Spheres	7-8	540	65
4	+, /	1	60	55

Table 3. Characteristics of snow used in the experiments.

Imaging and Stereological Analysis of the Snow Samples

CT Imaging Procedure. One of the snow samples was CT scanned prior to or very soon after beginning the experiment in order to get an initial image of the snow. After this, the samples were scanned approximately once per week. The CT scanning produces a horizontal cross-section of the specimen, and three images were taken at different vertical levels during each weekly scanning session. Each CT image is 16-bit (65,536 shades of gray), 1024 × 1024 pixels in size, and represents an actual area 102 cm square.

For the first two experiments, scans were taken at 3.5, 5.5, and 13.5 cm, measured from the bottom of the sample. Due to a large amount of settling, the scan at 13.5 cm was replaced with one at 7.5 cm for Experiment 4. Difficulties with the CT scanning equipment occasionally resulted in executing fewer scans. Since the snow samples could only be kept cold for a limited period of time, the majority of the scans were conducted in the bottom half of the specimen where the strongest faceting occurred, and only one scan was taken in the upper region. Snow specimens were kept frozen during the CT scanning process by packing them in a specially-designed container filled with dry ice (Figure 14). This canister attaches rigidly to the stage platform of the CT machine, eliminating any motion of the sample as it is scanned. The scanning process took about 2-3 hours per weekly session and can be assumed to have very little impact on the metamorphism process. All imaging was performed with a Synergistic Detector Designs CT scanner.

Figure 14. Chamber for keeping snow samples frozen during CT scanning.

Measurement of Snow Density From CT Images. One of the more important aspects of using CT technology to examine a snow sample is the ability to measure the density of the specimen from the CT image. Since the attenuation of the x-ray has a strong

dependence on density, the intensity of each pixel forming the CT image is essentially a measure of point density within the sample. This feature of CT technology was first utilized by Kawamura (1990) to measure the three-dimensional density of ice cores. From the value for each pixel (representing a shade of gray), a ratio can be formed relative to the pixel values for pure ice and air. Multiplying this ratio by the density of pure ice gives the density of the sample at a particular point. In equation form (Kawamura, 1990):

$$\rho_{sample} = \left(\frac{N_{air} - N_{sample}}{N_{air} - N_{ice}}\right)\rho_{ice}, \tag{15}$$

where:

N_{air} = Pixel value for air,

N_{ice} = Pixel value for pure, bubble-free ice,

N_{sample} = Pixel value for snow sample,

ρ_{ice} = Density of pure ice (917 kg/m^3), and

ρ_{sample} = Point density of snow sample.

The pixel values for the pure, bubble-free ice and air are determined by scanning samples of these constituents. Since the cooling chamber and specimen container also attenuate the x-rays, the configuration used while scanning the ice or air must be identical to that used while scanning the snow samples. Bubble-free ice contained in the same tapered cup used for the snow specimens was placed in the cooling chamber and CT

scanned at 3.5, 5.5, 7.5, and 13.5 cm above the bottom of the cup. This process was repeated with an empty cup to determine the pixel value for air.

For the purposes of this work, it is not necessary to calculate point densities of the sample but rather the average density over the entire two-dimensional slice. As a result, the average pixel value for the images were used for N_{air}, N_{ice}, and N_{sample}. This gives identical results as first determining the density at each pixel and then computing the average density. Table 4 gives the pixel values for pure ice and air at the different levels, as well as the resulting equation for computing the density of a snow sample.

Level (cm)	N_{ice}	N_{air}	Density Equation
13.5	175.49	5.73	5.40 N_{sample} -30.95
7.5	177.27	5.53	5.34 N_{sample} -29.55
5.5	177.93	5.66	5.32 N_{sample} -30.13
3.5	177.79	6.92	5.37 N_{sample} -37.14

Table 4. Pixel values for ice and air, and the resulting snow density equation, for each scanning level.

This procedure was tested on several samples of sieved snow of various densities. In each case, the average density was found by weighing the snow specimen and dividing by the known volume of the sample cup. This value was compared to the average of three density measurements calculated from CT images at different locations within the snow sample (Table 5). The densities obtained using both methods demonstrate strong agreement. The process of sieving the snow into the sample cup creates slight density variations that is evidenced by the deviation in the CT densities measured in a single

sample. Obviously, more scans of a particular specimen would give a better representation of the average sample density.

Test	CT Density	Average CT Density	Measured Density
1	260 248 234	247	253
2	256 291 285	277	268
3	363 356 343 352 356	354	348
4	68 63 59	63	63

Table 5. Comparison of densities computed from CT scans to measured values.

Converting CT Images to Binary. Before a CT scan can be analyzed by the microstructural measurement software, it must first be converted to a binary image where the snow grains are represented by black and the pore space is white. In order to convert an image to binary, a threshold value must be carefully selected; any pixel with a value

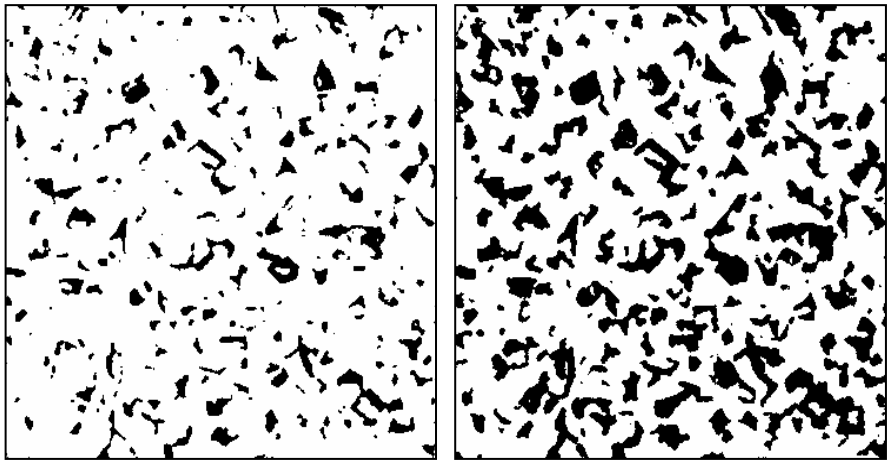

Figure 15. A CT image of faceted snow, converted to binary using two different threshold values.

less than the threshold becomes white and pixels with a greater value are turned black. Perla et al (1986) encountered problems in choosing a threshold value during the image analysis of serial sections. The choice of threshold value is extremely critical because it has a tremendous impact on the apparent density and structure of the snow, and will greatly effect any measurements made of the snow microstructure (Figure 15). Once the image is converted to binary, the density can be calculated based on the area fraction of black pixels which represent the ice grains. Taking advantage of this fact, a threshold value can be chosen that yields a density that is equal to that calculated directly from the CT image. While Perla et al (1986) recognized that a threshold value could be chosen to replicate the sample density, they did not have a method for measuring the density for each serial section and instead chose a threshold based on visual comparison to the original micrograph. This methodology obviously introduces a degree of subjectivity into what should be an objective, quantitative analysis.

The calculation of the average density for each two-dimensional CT image yields the key to creating an accurate binary representation in a completely objective manner. A macro was developed in Scion Image, an image analysis software similar to the Macintosh-based NIH Image, that automatically converts a gray-scale CT image to binary. First, a square region is selected from within the boundaries of the sample cup. A median filter is performed to clean up the image and render it more suitable for stereological analysis. From the average pixel value within the selected region, the macro computes the density using the procedure outlined in the previous section. Finally, a threshold value is chosen to match the calculated density and the image is converted to binary.

Measurement of the Snow Microstructure. Once a binary image of the snow sample was obtained, the image was analyzed using an automated stereology software. For a detailed description of the stereology theory and how it is utilized to measure the microstructure of snow, see Edens and Brown (1994). From the binary image, the program calculates a multitude of parameters describing the grains, bonds, and pore space, outputting both the mean value as well as the standard deviation. Of particular interest to studies of snow microstructure are grain radius, intercept length, volume-weighted-volume (VWV), bond radius, and neck length.

One important measure that is not calculated satisfactorily by the software is the snow grain size. The grain radius that is computed is based on the radius of the largest circle that can be inscribed into the snow grain. In nearly all cases, this significantly

underestimates the grain size as measured by standard observation procedures. However, the stereology program also calculates the mean intercept length and the volume-weighted-volume, which are both indicative of the size of the snow particle. To determine a mean grain size from the intercept length, the following equation is used:

$$r_g^{intercept} = \frac{2}{3} N_L , \tag{16}$$

where N_L is the mean intercept length. The volume-weighted-volume gives a measure of the average grain volume, giving more weight to particles with larger volumes. By determining the radius of a sphere occupying a volume equivalent to the calculated volume-weighted-volume, a representation of grain radius can be found:

$$r_g^{VWV} = \sqrt{\frac{3 \cdot VWV}{4\pi}} . \tag{17}$$

In practice, the grain radius is usually doubled to obtain the grain size.

Since snow subjected to a strong temperature gradient develops a significant degree of anisotropy in the vertical direction, it should be noted that the measurements pertaining to the grains and bonds are valid only for the snow contained in the horizontal CT section that is analyzed. By performing horizontal CT scans at several different heights through the snow sample, variation of the snow microstructure in the vertical axis can be ascertained.

Temperature and Vapor Pressure Gradient Calculations

From the daily temperatures recorded within the sample cup, the average temperature gradients were calculated for the vertical intervals 0-4, 4-8, and 8-12 cm

(measured from the bottom of the cup). The vapor pressures at the 0, 4, 8, and 12 cm levels in the snow sample were calculated using the Goff-Grattch formulation obtained by integrating the Clausius-Clapeyron equation (List, 1949; Birkeland et al, 1998):

$$log_{10}(e_i) = -9.09718\,(\frac{T_o}{T} - 1) - 3.56654\ log_{10}(\frac{T_o}{T}) + .876793\,(1 - \frac{T}{T_o}) + log_{10}(e_{io}) \quad , \qquad (18)$$

where:

e_i = saturation vapor pressure of a plane surface of pure ordinary water ice,

T = absolute temperature (deg K),

T_o = ice-point temperature (273.16 deg K), and

e_{io} = saturation pressure of pure ordinary water ice at ice-point temperature (6.1071 mbar).

Finally, the average vapor pressure gradients were calculated over the same intervals as for the temperature gradients.

CHAPTER 4

RESULTS AND DISCUSSION

Comparison of SNOWPACK Results to Field Observations and Measurements

Prediction of Snow Depth

The graphical user interface provides a convenient means to view the results of the SNOWPACK model. Figure 16 shows how the calculated snowpack depth compares to

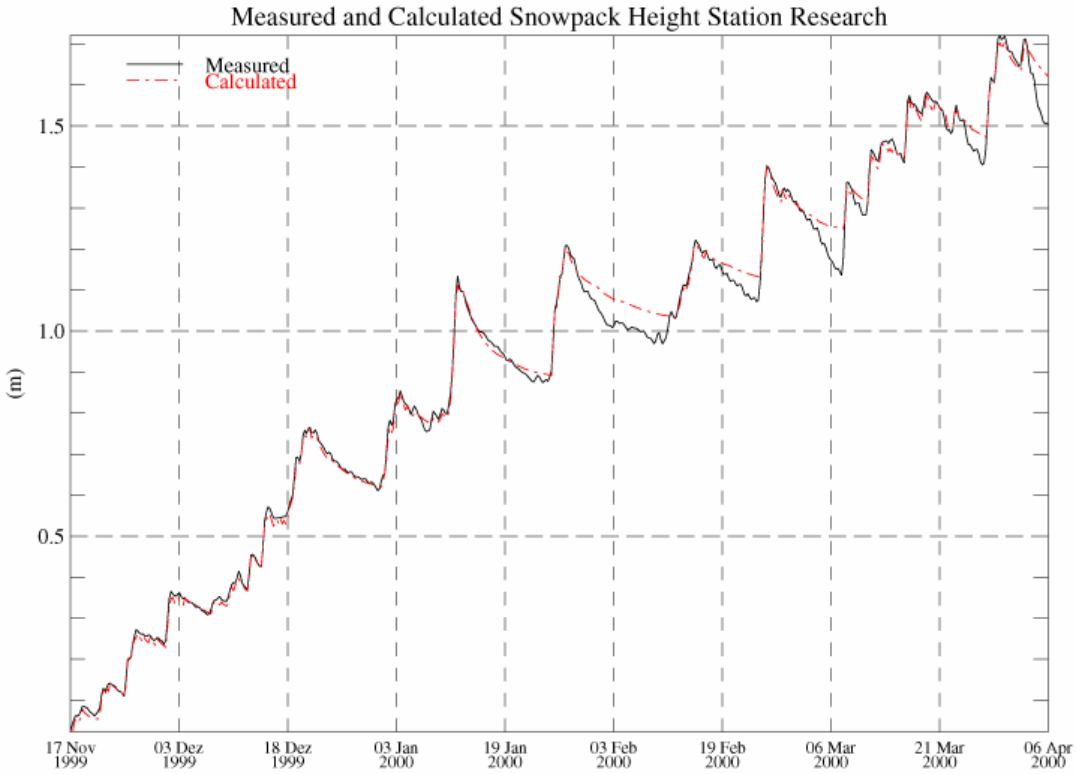

Figure 16. Output from the SNOWPACK graphical user interface showing modeled and measured snowpack depth over the course of the winter.

the depth measured ultrasonically at the weather station. Until the end of January, SNOWPACK predicts the settling rate quite accurately. The model adds new snowfall when appropriate, and the predicted settling curves closely match the measured ones. However, by the end of January, the model consistently underpredicts the settling rate. As a result, the calculated and measured snow depths become increasingly divergent until a new snowfall event sets the two equal. In the early winter, small snowfall events occurred frequently so that the modeled snow depth was reset to the measured depth relatively often. Towards spring, snowfall came less frequently, and as a result, SNOWPACK must predict the snowpack depth for longer periods of time until new snowfall occurs. Another explanation of the increasing disparity between the modeled and measured snowpack depth is that by February, the snowpack is receiving much more energy input from solar radiation. This effect may have been further augmented by the surrounding terrain features. For the early part of the winter, much of the direct sunlight was blocked by a low ridge to the south of the site, but by February the sun was able to clear the ridge, resulting in a large increase in solar exposure in a short period of time. The timing of this discrepancy between predicted and actual settling rates could indicate a need to improve the relationship between incoming shortwave radiation and the calculated settling rate, or an improved estimation of the snow surface albedo.

Throughout the winter, snow depth at the field station was recorded using three separate methods. Using an ultrasonic depth gauge mounted on the instrument tower, the depth of the snow cover was logged on 30 min intervals throughout the winter. In addition, the snow depth was recorded during the weekly visit to the site both in the

snowpit and from markings on the thermocouple array. With a few exceptions, these depths correlate well (see Table 6). This is an important consideration and allows the snowpit observations and temperature data to be compared to the model output with a minimum of spatial variation.

Date	Thermocouple Array	Ultrasonic Depth Gauge	Snowpit
11/30/99		24	24
12/10/99		37	39
12/16/99	55	56	58
12/21/99	75	68	
12/30/99	62	62	63
1/7/00	76	75	78
1/13/00	106	105	110
1/20/00	90	92	92
1/27/00	117	116	127
2/3/00	101	101	102
2/10/00	101	97	104
2/17/00	115	118	116
2/24/00	106	106	106
3/2/00	126	126	129
3/9/00	131	130	132
3/16/00	141	140	142
3/23/00	146	147	147
3/30/00	170	170	170
4/6/00		150	156

Table 6. Comparison of snowpack depths (cm) measured using three different methods.

Prediction of Snowpack Layering

Figure 17 gives an effective visualization of how the layering of the simulated snowpack evolves throughout the course of the winter by plotting grain type versus depth and time. Layering present in the modeled snow cover are visually compared to snowpack observations from the field site in the following discussion.

Surface Hoar and Near-Surface Faceted Layers. The most striking features of the modeled layering (Figure 17) are the two surface hoar layers that originate on

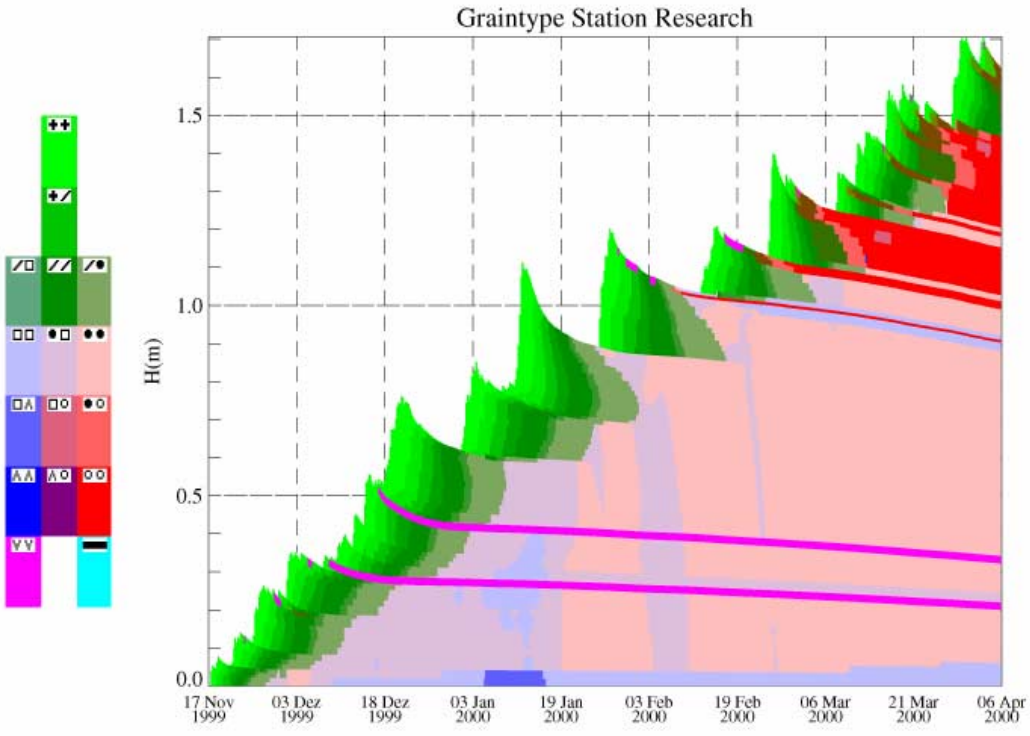

Figure 17. Output from SNOWPACK model illustrating simulated grain type versus time and height above the ground.

approximately 9 December and 17 December, and persist the entire winter. The surface hoar prediction routine in SNOWPACK is still under development, and at the present time the model seems to significantly overpredict its occurrence (Pielmeier et al, 2000). Although neither of these two prominent layers correspond to actual surface hoar observed in the field, the layers do match very well with two near-surface faceted layers observed early in the winter. The first near-surface faceted layer was observed buried at a depth of 30 cm above the ground on 16 December. This layer continued to be evident between 20 and 30 cm above the ground until 2 March. The originating date of a second layer of near-surface facets is hard to pinpoint, but the layer was observed from 7 January to 2 March at heights between 30 and 40 cm. Since the conditions necessary for the formation of near-surface facets and surface hoar crystals are similar, it is not surprising to find the correspondence between the two layers. While SNOWPACK also predicts a layer of mixed facets and rounds associated with the lower surface hoar layer, they are not true near-surface facets since they did not form until the layer is buried. No facets are modeled in conjunction with the upper surface hoar layer. Additionally, both layers of surface hoar and the layer of mixed facets and rounds persisted the entire season, whereas in the field, they had become completely rounded by 2 March.

Two instances occurred where SNOWPACK correctly predicted the formation of surface hoar. On 17 February, a developing layer surface hoar was observed on the snowpack surface, and was simulated by the model as well. SNOWPACK predicted its destruction only a few days later; indeed, it was not found during the field study on 24

February. Again on 2 March, surface hoar was both observed and predicted by SNOWPACK.

Snowpack simulated surface hoar on at least five other occasions, but since no field observations were made on corresponding days, it is not known if these predictions are correct.

Rounding and Faceting of the Snowpack. Perhaps the most important function of the SNOWPACK model is to accurately simulate the metamorphism of the snowpack, both towards faceted and rounded forms, since this mechanism has a profound effect on the strength and stability of the snow cover.

The model simulates the strongest faceting to occur at the base of the snowpack, which is consistent with observation. SNOWPACK predicts that pure facets will be present in the bottom 5 cm from the beginning of December until the end of the study period. While fully faceted crystals were found at the snowpack base at the beginning of the winter, they were observed as mixed rounds and facets by 30 December, and completely rounded by 9 March. Furthermore, cup-shaped depth hoar crystals were noted at the base of the snow cover once on 10 December, but depth hoar was only predicted by SNOWPACK for a short period in early January.

Through the majority of December, the observed snowpack consisted primarily of rounded facets beneath decomposing and recent precipitation forms. By the beginning of January, a layer of rounded grains had formed between 50-60 cm. From then until 9 March, the resulting snowpack architecture was largely three-tiered: mixed forms from

about 40 cm down, overlaid by a layer of strong, rounded snow, and finally new and decomposing precipitation particles at the top. This prominent layering is not evident in the model output. The simulated snowpack consists of a basal faceted layer, mixed forms, and decomposing new snow through mid-January, with no completely rounded layers. However, around 19 January, SNOWPACK predicts that the majority of the mixed rounds and facets become entirely rounded rather suddenly.

During a period of warm, clear weather occurring the first week in February, the model predicts surface melting and a resulting layer of wet grains at a height of 1 m. It seems as if this wet layer develops a temperature gradient that forms an adjacent layer of faceted grains, which persist for the rest of the study period. Neither actual surface melting or faceted grains were observed at the field site as a result of this weather event.

One interesting phenomena that can be observed in the model output is the abrupt onset of faceting, and then a return to the original crystal type. This occurs on three separate occasions: 4 January, 1 February, and 19 February. In the first instance, a region of mixed forms centered around 30 cm above the ground becomes completely faceted and then abruptly returns to mixed forms. During the same time period, the faceted snow at the base exhibits some formation of depth hoar. An even more pronounced change occurs starting on about 1 February, with a region from 5 to 80 cm metamorphosing from rounds to mixed forms, then back again, over the course of about 3-4 days. A similar event takes place starting 19 February, and is even shorter lived. Referring to the simulated snowpack temperatures illustrated in Figure 18, no remarkable temperature gradients occur during these events to drive any significant kinetic-growth

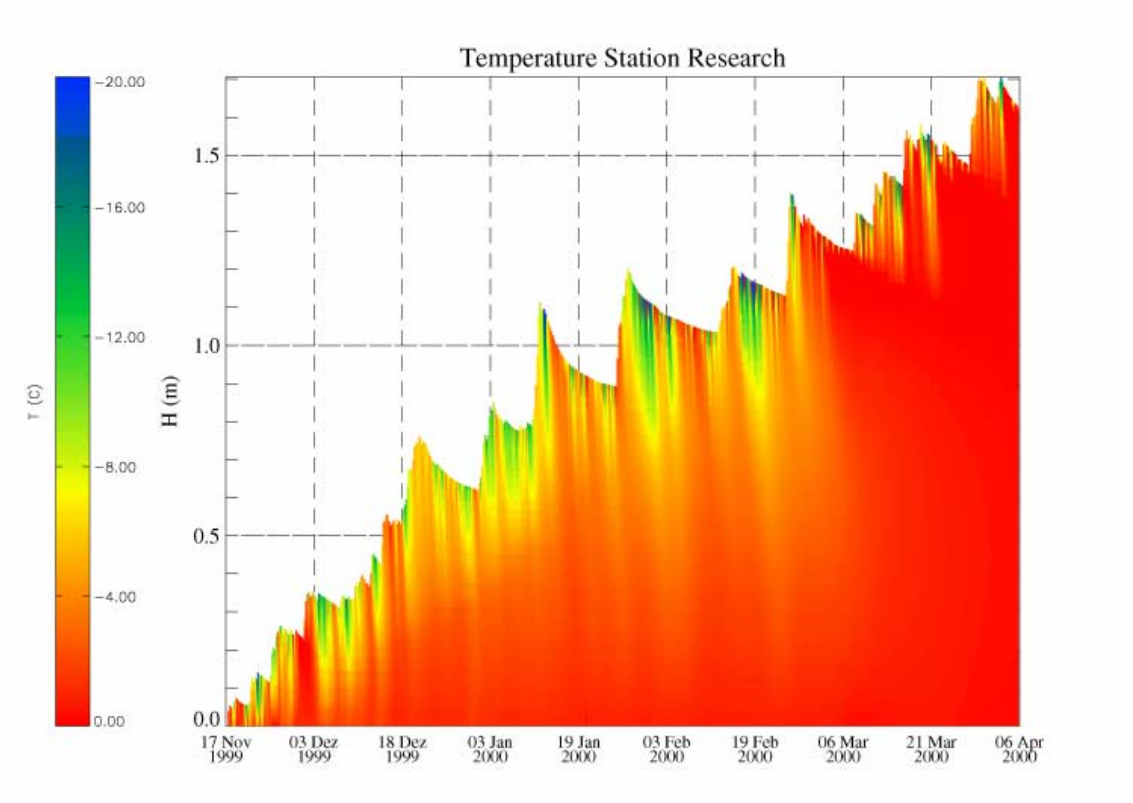

Figure 18. Predicted temperature plotted against time and height above the ground.

metamorphism. It is unlikely that these occurrences correspond with any physical processes within the actual snowpack, but rather stem from problems with the SNOWPACK program.

Although some of the variation between the modeled and observed data are a result of model inaccuracy, observing the differences between facets, mixed forms, and rounded grains can be quite subtle, and this may account for some of the discrepancies between the simulated and observed snowpack.

Melt-Freeze Layers. While SNOWPACK does not specifically predict melt-freeze grains or crusts (Class 9), it may be inferred that layers that the model predicts as wet (Class 6) are likely to become melt-freeze crusts if their temperature drops below freezing. Therefore it is reasonable to compare melt-freeze crusts observed during the field studies to wet grain layers simulated by SNOWPACK, denoted by the red color in Figure 17.

The first wet layer modeled by SNOWPACK originates in mid-February, but no corresponding feature was noted in the field. A melt-freeze crust observed just below the snow surface on 24 February was correctly predicted by the model. The following week, on 2 March, this crust was still present in both the observed and simulated profiles, but now buried by over 20 cm of new snow. Additionally, another crust was observed on 2 March just below the surface, and again it was accurately modeled by SNOWPACK. For the next two weeks, these three crusts were evident both in the model and observations, with no new melt layers developing. During the remaining three weeks of the study period, SNOWPACK predicts the formation of a variety of melt layers, and eventually a large portion of the upper third of the snowpack becomes wet. Although a number of new melt-freeze crusts are noted in the field from 23 March through 6 April, the observed crusts were thin and separated by dry snow. Since SNOWPACK does not accurately predict the depths of these layers, due to inaccurate estimation of the spring-time settling rate, it is difficult to make any direct comparisons of the modeled and observed melt-freeze crusts during this time period.

Statistical Comparison of SNOWPACK Results to Snowpit Observations

A comparison of the field notes to the graphical output of SNOWPACK is useful since this visualization of the simulated snowpack is the primary interface between the model and the human user. However, in order to more accurately ascertain the effectiveness of the SNOWPACK model, a more rigorous and objective analysis is necessary. The use of standard statistics, as outlined in CHAPTER 3 – METHODOLOGY, provides a means for accomplishing such a task.

As discussed in the previous section, the surface hoar prediction routine in the SNOWPACK model is still under development and tends to overpredict the occurrence of surface hoar. This was acceptable when making a visual comparison of the model output to the snowpit notes, but produces erroneous results during a numerical analysis. The surface hoar layers simulated by SNOWPACK are typically small grained (less than 0.5 mm) and of low density (100 kg/m^3), and up to five of these layers are allowed at any given time. Since these surface hoar layers do not always exist in reality, the resulting data points significantly alter the statistical measures and prevent an accurate statistical evaluation of the model. To eliminate this problem, the surface hoar routine was disabled for the numerical comparison.

Additionally, one outlying data point was removed from the analysis. The layer originated on 28 February as new snow fall; shortly thereafter the layer became wet and the grain size began increasing, finally reaching a value twice that of any other grain size simulated by SNOWPACK. During this same period, the density decreased dramatically from 140 kg/m^3 to 70 kg/m^3, and then increased to 130 kg/m^3. The resulting layer coincided with data from a snowpit performed on 6 April, and the outlying data point is

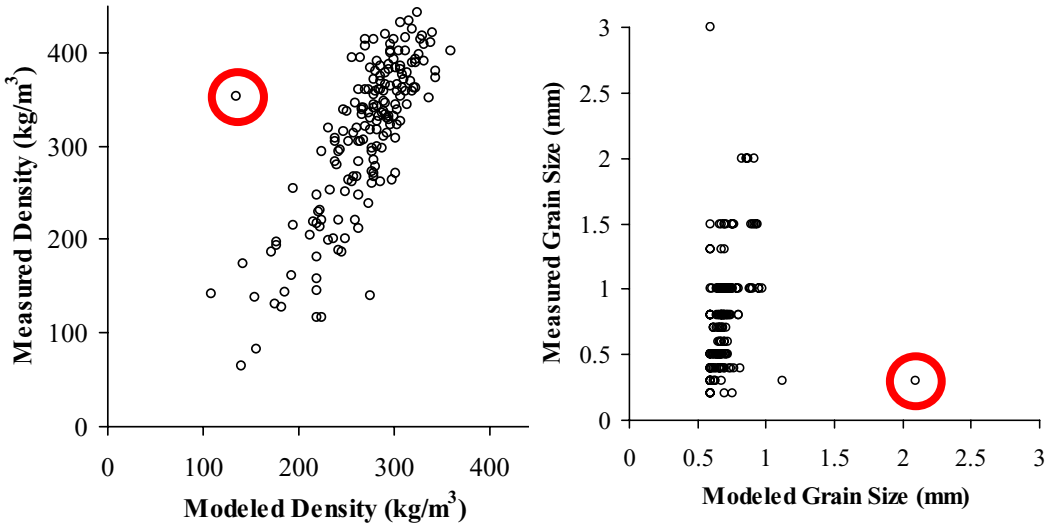

Figure 19. Outlying data point shown in graphs of density and grain size.

show in Figure 19. Since this point significantly lowers the statistical values for both density and grain size, it was eliminated from the analysis. With this outlying data point removed, the statistical analysis more realistically reflects the performance of the SNOWPACK model.

Results of Statistical Analysis. Table 7 gives the results of the statistical procedures performed for the five numeric parameters that are both calculated by SNOWPACK and measured during the field studies.

	Data Pairs	Error	Correlation	Linear Regression		
Parameter	***n***	***MSE***	***r***	**Intercept**	**Slope**	R^2

Temperature (deg C)	199	1.06	0.87	-0.44	0.86	0.76
Temp. Gradient (deg C/m)	157	11.43	0.39	2.99	0.16	0.15
Density (kg/m^3)	177	66.51	0.83	-112.87	1.56	0.69
Grain Size (mm)	179	0.41	0.44	-0.69	2.12	0.19
Grain Size (Normalized)	179	0.18	0.44	0.13	0.39	0.19

Table 7. Results of the stastistical procedures for parameters measured on a continuous, numeric scale.

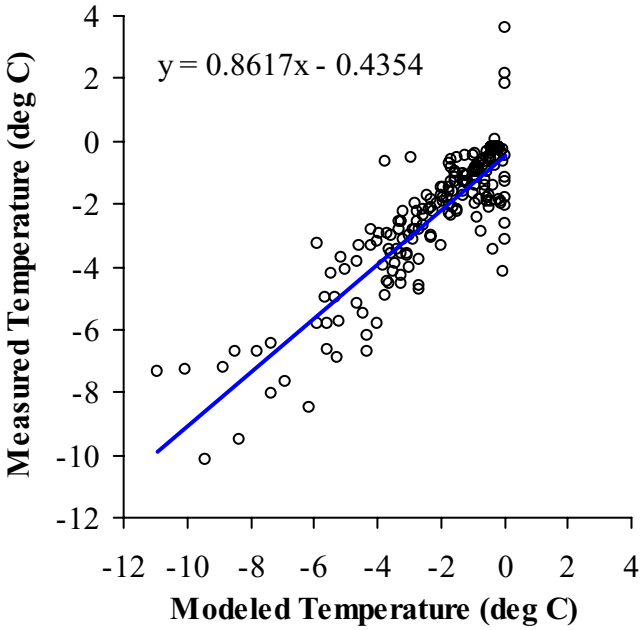

Figure 20. Linear regression of the modeled temperatures on the measured temperatures.

Temperature. It is apparent from the results in Table 7 that temperature is modeled accurately by SNOWPACK. The mean squared error (MSE) is only 1.06 deg C, indicating that the predicted snowpack temperatures are usually quite close to the measured temperatures. Additionally, a strong positive correlation exists between the

simulated and actual values, with the Pearson's correlation coefficient approaching one. Further support of SNOWPACK's accurate calculation of snowpack temperatures is evidenced by the linear regression analysis (Figure 20). The intercept is only -0.44 deg C, which is close to the optimum value of zero, and the slope is nearly one. Furthermore, a high R^2 means that a large percentage of the data points fall near the regression line.

Figure 21 shows the modeled and measured snowpack temperatures as a function of time over the winter for three different depths. In general, for each location within the snowpack, the temperatures predicted by SNOWPACK are fairly similar to those measured. This provides additional qualitative evidence that the model is able to effectively predict the temperatures within the snowpack. The graphs presented in Figure 22 also demonstrate a close correlation between the predicted and measured temperatures, but reveal that the accuracy of the model diminishes slightly near the snowpack surface. On 6 April, it is apparent that SNOWPACK predicts isothermal snow in the upper 40 cm of the snowpack, while in actuality, the snow is either not wet or refrozen since the measured temperatures are significantly lower in this region.

The high degree of accuracy obtained by SNOWPACK in modeling the temperature profile of the snow cover indicates the use of a successful thermal conductivity model, but also is a result of knowing boundary temperatures at the snowpack base and surface. Additionally, the accuracy of the model may point to the effectiveness of integrating snow microstructure into the thermal conductivity formulation. However, SNOWPACK does encounter some difficulties predicting upper-snowpack temperatures, especially in

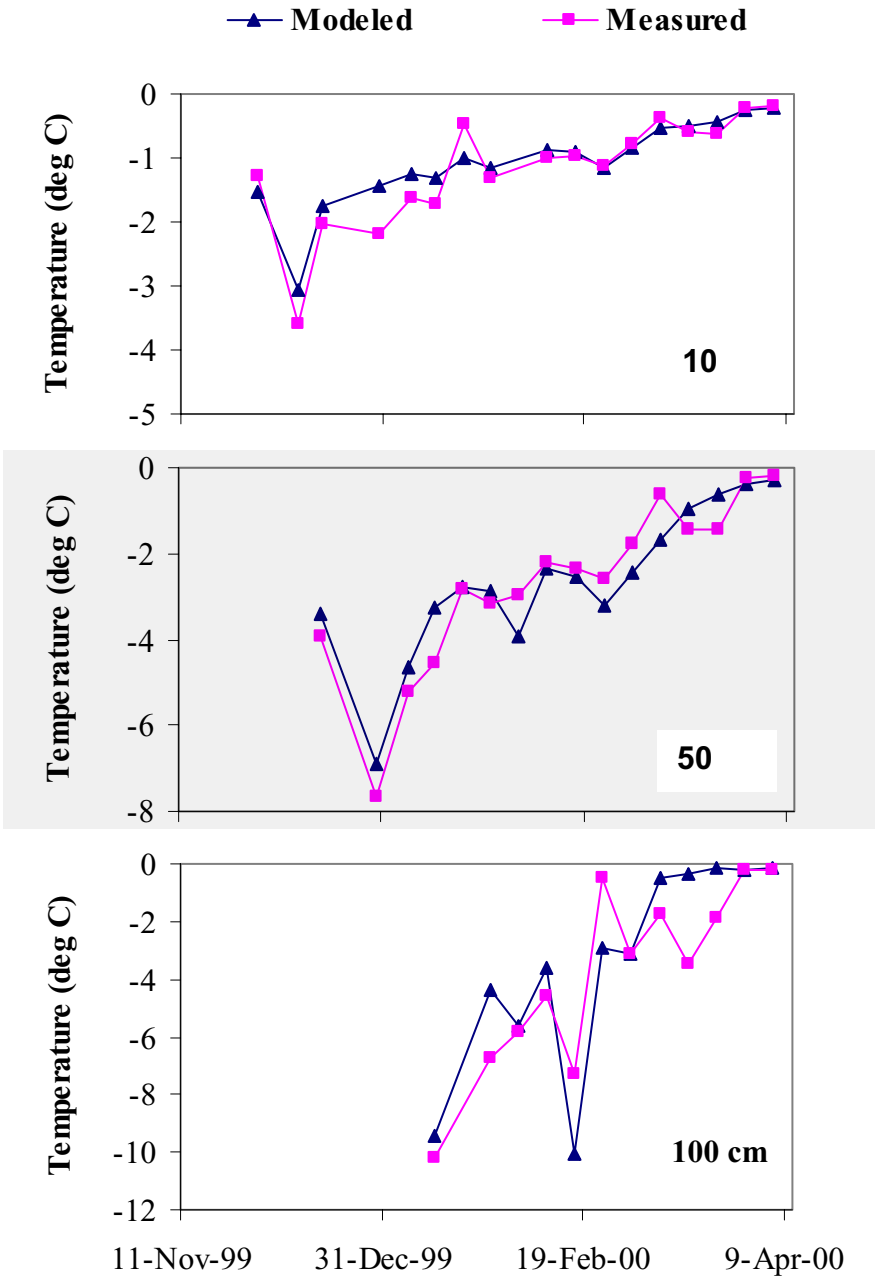

Figure 21. Modeled and measured temperature plotted against time for 10, 50, and 100 cm above the ground.

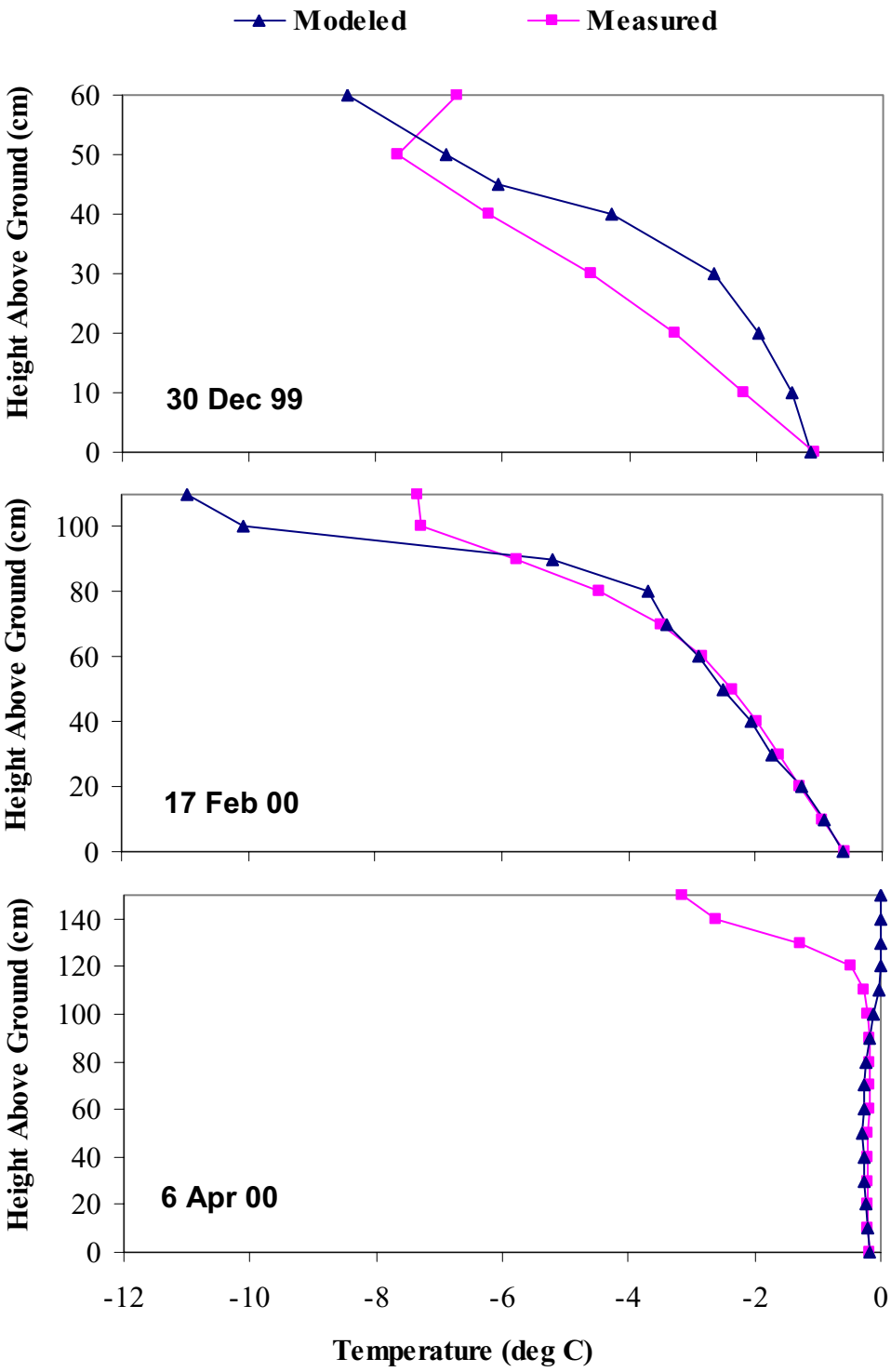

Figure 22. Modeled and measured temperature versus snowpack depth for three different dates.

the spring. Effective simulation of the energy exchanges at the snowpack surface is only possible if the albedo and extinction function are predicted accurately; these relations may need some refinement. The difficulties encountered in the spring are likely a result

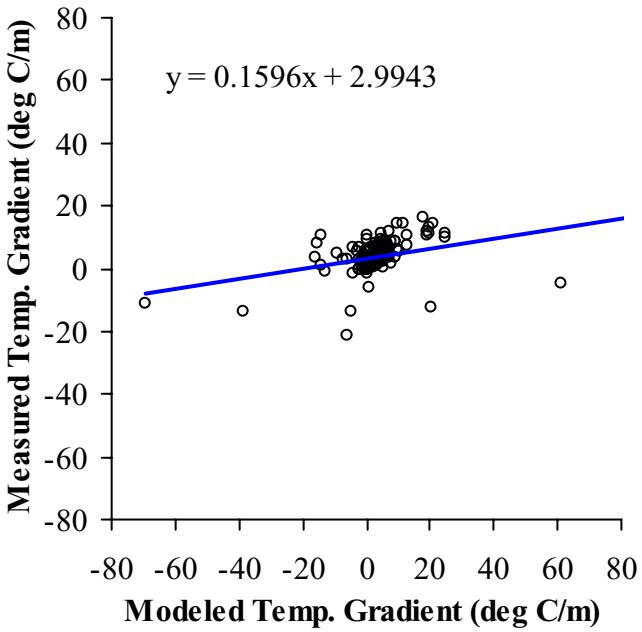

Figure 23. Linear regression of the modeled temperature gradient on the measured temperature gradient.

of the inability of the model to realistically simulate the melting and refreezing of the snowpack, stemming from an incomplete treatment of wet snow metamorphism.

Temperature Gradient. Effective simulation of the thermal gradients are essential since they play a dominant role in snow metamorphism. The success of the SNOWPACK model in predicting the temperature profile within the snowpack would seem to imply

that the calculated temperature gradients will also be accurate. However, numerical differentiation of the temperatures in order to calculate the gradients will introduce noise and error. The variation in temperature must follow a function that is restricted by the boundary conditions at the snowpack base and surface, but without such a function defining the temperature gradient, more fluctuation is allowed.

The statistical measures for temperature gradient (Table 7) are not nearly as high as for temperature, and are actually quite low. The MSE of 11.34 deg C/m shows that the predicted values for temperature gradient are generally not very close to the measured values. The R^2 for the regression is very low, representing a large degree of scatter in the data (Figure 23), and the regression slope of 0.16 is also much smaller than the optimal value of one. The Pearson's correlation coefficient is the strongest of the statistical measures, but is the lowest of all the modeled variables at 0.39.

Several outlying points visible in Figure 23 seem to significantly skew the regression line, and likely affect the other statistical measures as well. The bulk of the data points fall within the interval between –10 and 10 deg C/m, and appear to be clustered near a line with a slope close to one. In contrast, the more extreme temperature gradient values exhibit a higher degree of scatter. To address this variance, the statistical tests could be applied to small and large temperature gradients independently, or alternatively, to temperature gradients found in the upper and lower snowpack. Dividing the data set may reveal where SNOWPACK has the most difficulty predicting temperature gradient.

To complicate the comparison of modeled and measured temperature gradients, several sources of error exist that are likely to influence the analysis. SNOWPACK does

not output the predicted temperature gradients directly, so they must be calculated according to the method presented in CHAPTER 3. Additionally, these calculated values are then interpolated to obtain temperature gradients at the appropriate levels. The same holds true for the measured temperature gradients; these must also be computed from the temperatures measured in the field. The comparison of two secondary quantities is bound to incur some amount of error. So even though the statistical analysis comparing the simulated and measured temperature gradients gives generally poor results, potential flaws in the analysis prevent any meaningful conclusions from being drawn regarding the model's ability to simulate the temperature gradients.

Density. Referring again to Table 7, it is evident that the SNOWPACK model has some difficulty accurately simulating snow density. The MSE is quite large, 66.51 kg/m^3, and further analysis reveals that SNOWPACK underpredicts the snowpack density on more than 80% of the data. This is further evidenced by a negative regression intercept of –112.87 kg/m^3, and a slope of 1.56 (Figure 24). Of particular interest is that the vast majority of instances where SNOWPACK overpredicts the density occur in the upper regions of the snow cover, leading to the conclusion that the model predicts new snowfall densities that are too large. Even though the modeled density is too low the majority of the time, the R^2 for the regression is reasonably high, and the correlation coefficient of 0.83 is only slightly lower than the Pearson's r for temperature.

Figure 25 shows that similar trends are present in modeled and measured time-series graphs of density for three different snowpack depths. It is important to note that for the

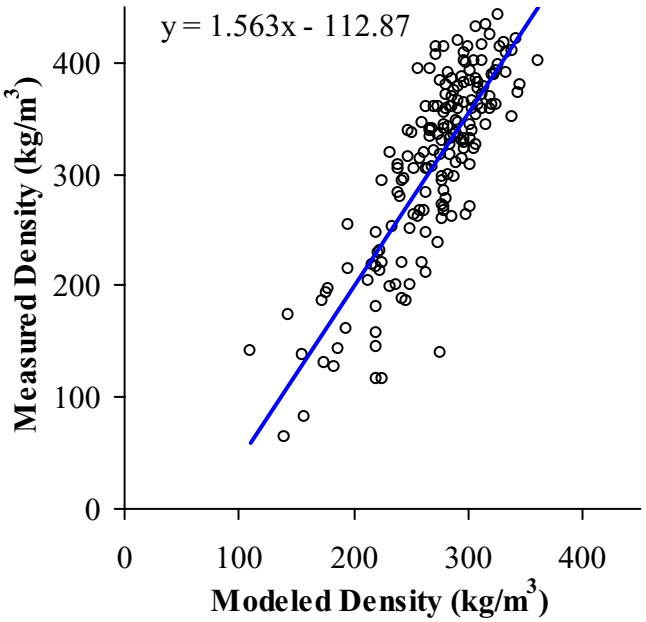

Figure 24. Linear regression of the simulated snowpack density on the measured density.

first half of the winter, SNOWPACK actually overpredicts the density at 100 cm above the ground. Since the 100 cm level was close to the snow surface during this first portion of the winter, additional evidence is provided that SNOWPACK overpredicts new snowfall density. Figure 26 shows the variation in density with height for three different times during the winter. In each case, the modeled and measured densities follow similar curves, but are generally offset, especially in the bottom two-thirds of the snow cover. Since there was new snowfall just prior to 17 February, SNOWPACK predicts densities in the upper regions of the snowpack that are too large. While this behavior is not observed on 30 December, there had not been any recent new snow. It is evident that on 6 April, the model underpredicts the density through the full depth of the snow cover.

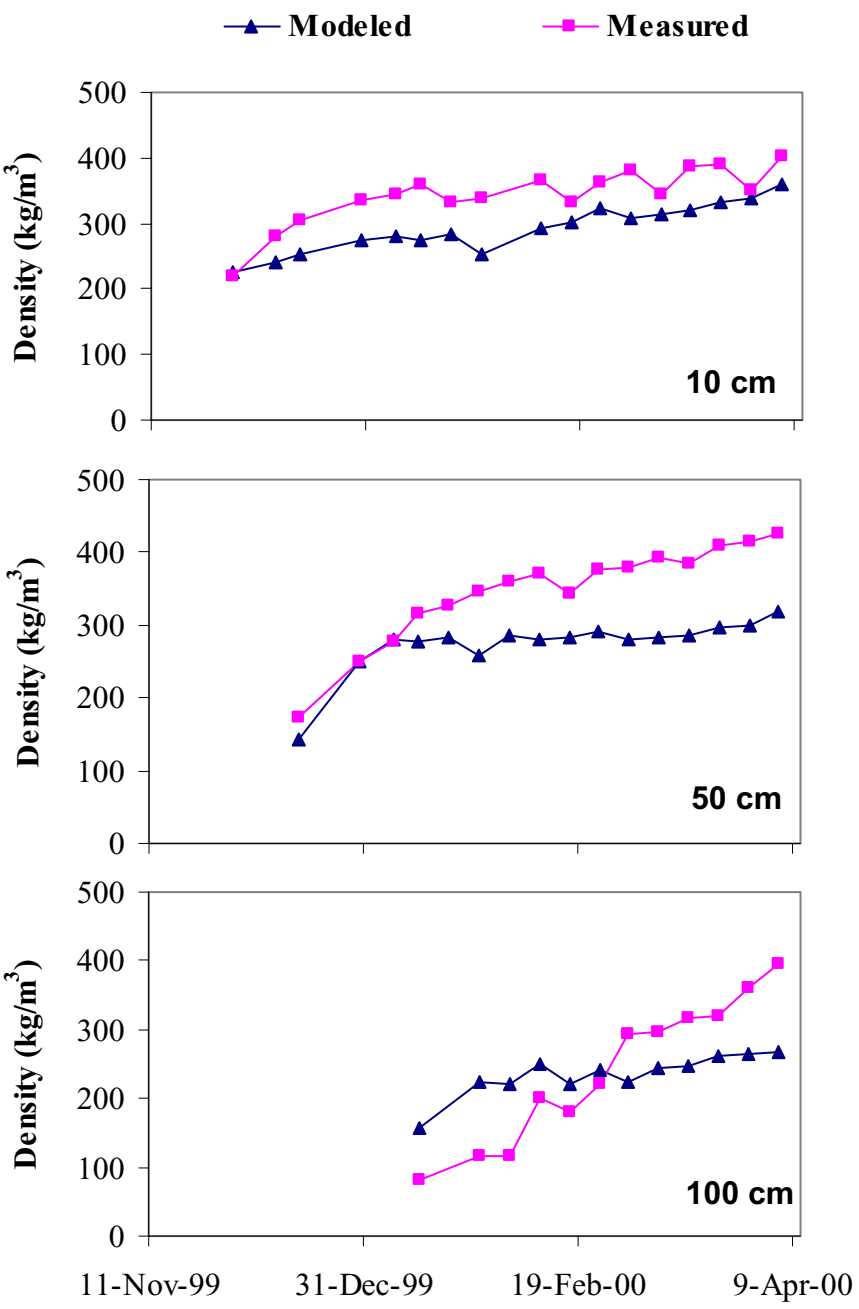

Figure 25. Modeled and measured density plotted over time for 10, 50, and 100 cm above the ground.

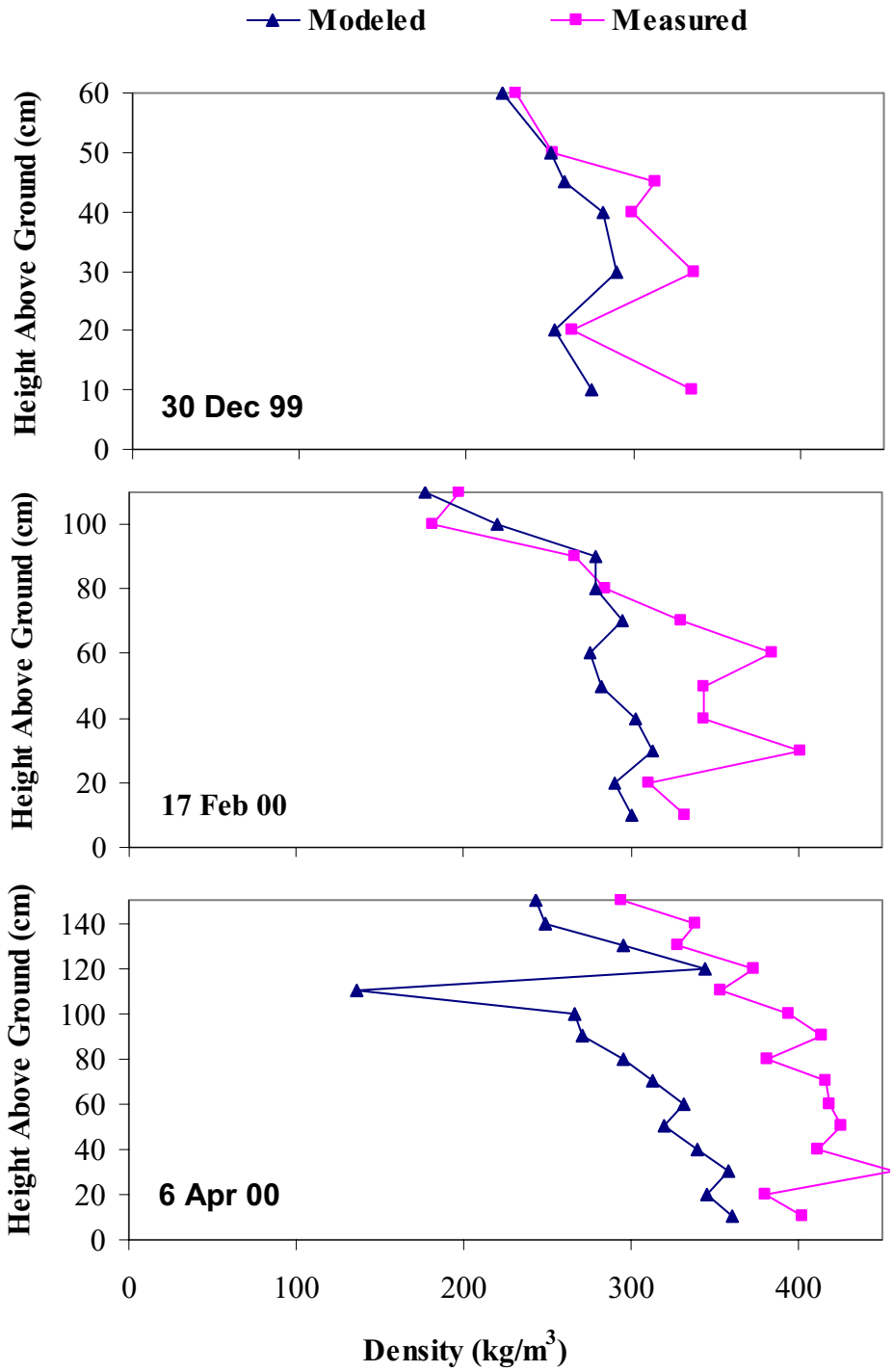

Figure 26. Modeled and measured density versus snowpack depth for three different dates.

It seems that SNOWPACK is able to predict the trends in density with some degree of accuracy, but falls short in calculating the actual value, underestimating the magnitude the majority of the time. Although flaws in the viscosity formulation could be responsible for the errors in density encountered in this analysis, the viscosity model has been compared to experimental data with positive results (Brown, personal communication, 2000). A more likely explanation could be incorrect calculation of grain and bond growth, which significantly affect the viscosity (Equation 1). The growth rates for these variables are governed by the equilibrium and kinetic-growth metamorphism laws, which have not been extensively validated. In contrast, for the case of new snowfall, the model consistently chooses a precipitation density that is too large. The precipitation density is found through an empirical relation based on meteorological parameters, and may be biased towards climatic conditions found in Switzerland.

Grain Size. All of the statistical measures comparing the original grain size data gave poor results. The MSE reveals that the modeled and observed grain sizes differ by an average of 0.41 mm. The R^2 for the linear regression is very low, and it is apparent from Figure 27 that the data points are scattered. The intercept of the regression line is -0.69 mm, and the slope is steep at 2.12. The strongest of the statistical measures is the correlation coefficient of 0.44, which is still lower than the other parameters but indicates at least some correlation between the predicted and observed grain size.

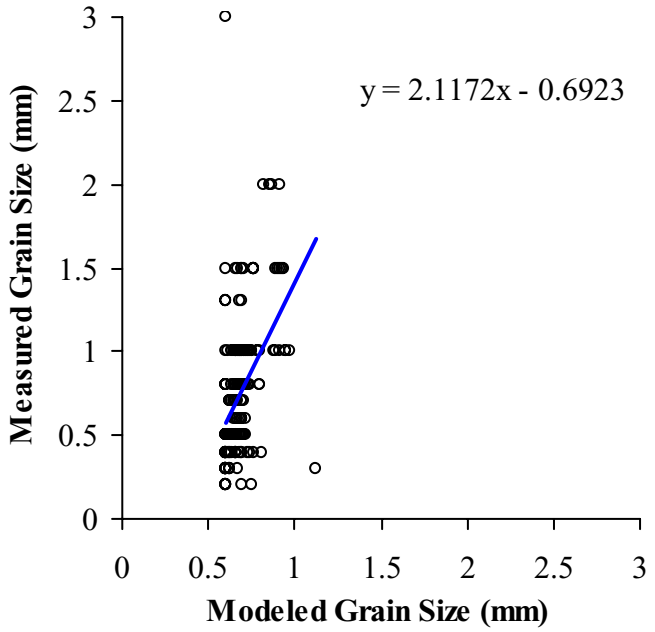

Figure 27. Linear regression of the predicted grain size on the observed grain size.

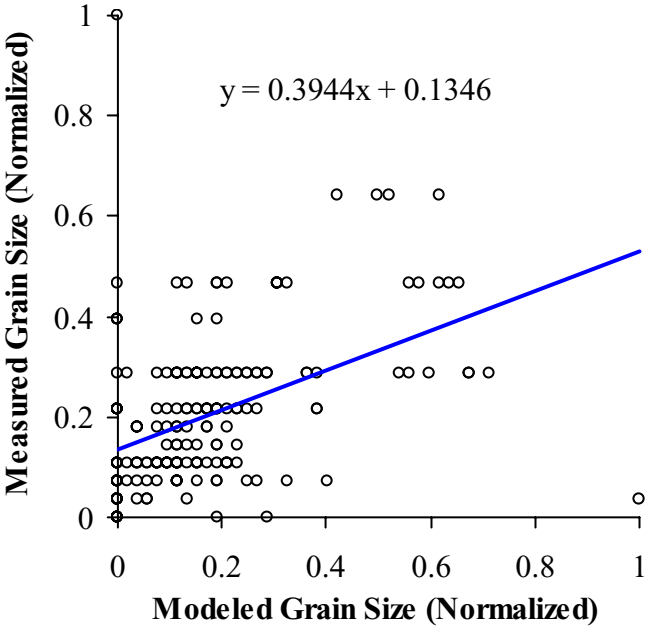

Figure 28. Linear regression of the normalized modeled grain sizes on the normalized observed values.

If sizes are normalized, the MSE and Pearson's *r* exhibits little change; however the linear regression shows some improvement. While the R^2 is still low, the intercept increases to 0.13, and the slope flattens to 0.39.

Grain size is undoubtedly the most subjective of the observations made during the field study, and the unimpressive statistical results comparing the modeled and observed grain sizes are probably not as negative as they may seem. As discussed in CHAPTER 3 - METHODOLOGY, the definition of grain size used by SNOWPACK and field observers can be very different. In contrast to temperature and density field measurements, the grain size as measured by a subjective observer does not provide a very reliable baseline to which the model data can be compared. A normalization of the grain size was performed to minimize this effect, but did not significantly affect the analysis. As a result, the statistical analysis does not provide very meaningful conclusions regarding the performance of the model in predicting grain size, but may underscore the necessity of developing a more standardized measure of grain size.

Although the subjectivity of grain size measurement in the field is surely one source of error, some problems within SNOWPACK are probable as well. Predicting grain growth during equilibrium and kinetic-growth metamorphism is a complex task, and the theories used by SNOWPACK have not been extensively validated (Brown, personal communication, 2000). Another possible problem lies in the assignment of the initial grain size of new snow, which is always defined as 0.6 mm. Since the model only allows grain growth, no grain sizes less than this initial value are ever predicted. However, grain sizes less than 0.6 mm are routinely observed in the field. Quite often, faceted snow that

is beginning to round is often observed in the field to decrease in grain size; once again, only grain growth is permitted in SNOWPACK.

Comparison of Modeled and Observed Grain Type

Similar to grain size, observation of snow cystallography is not an exact process, and as such, is subject to the differences in technique and skill of the observer. Furthermore, the crystal shape is not defined in a continuous, numeric format and must be analyzed using different statistical techniques. In CHAPTER 3, a methodology was presented that combined a X^2 statistical test with a proprietary agreement measure in order to allow a reasonably objective comparison of the modeled and observed grain shape.

The results of the X^2 test are summarized in Table 8. Cramer's Φ provides an estimate of the amount of similarity between the modeled and observed grain types, and is interpreted in the same fashion as Pearson's *r*. Both of the Φ values for the majority and minority crystal types are quite similar, but low. This indicates that the degree of correlation between the predicted and observed grain types is not very strong.

	n	**X^2**	**Cramer's Φ**
$F1$	198	112.59	0.38
$F2$	198	107.17	0.33

Table 8. Results of the categorical statistical measures used to evaluate the grain classification.

Using the second analysis method devised by Lehning et al (2000), a distance measure for crystal type, d_{type}, was calculated to be 0.27. While this value is similar to the Cramer's Φ, they cannot be directly compared since d_{type} has a theoretical range of 0, for no error, to 1, representing complete disagreement between modeled and observed crystal shape. While there are no hard-and-fast rules for interpreting this figure, a value of 0.27 seems to imply a significant amount of correspondence between the predicted and observed cystallography, which stands in contrast to the statistical results.

The difficulty in comparing the grain type calculated by SNOWPACK to crystal shapes observed in the field (or laboratory) seems to point towards the need for some common ground in the characterization of snow crystallography. A first source of complication, as well as error, arises when the model assigns a crystal type based on various combinations of the proprietary grain shape parameters, sphericity and dendricity. However, since there are no guidelines for quantifying sphericity and dendricity during field observations, bypassing the ISCI grain classification is not possible at the present time. Fierz and Baunach (2000) encountered similar difficulties when comparing laboratory and field grain type measurements to those predicted by SNOWPACK, and explored an alternative, improved grain shape parameter termed "zero curvature." While zero curvature is promising as it is can be directly computed by image analysis software, it is still not applicable to field observations unless disaggregated snow crystals are brought back from the snowpit site. While field observation of crystal type is unavoidably subjective, the development of a new shape parameter, one that is both calculated by the

model and can be readily quantified in the field, would greatly augment the utility and validation of the SNOWPACK model.

Sources of Error in the Analysis.

Despite the objectivity of using a statistical analysis to evaluate the SNOWPACK model, potential sources of error still exist that merit discussion. The causes of possible error fall roughly into one of three categories:

1. Instrumentation and measurements,
2. Human observations, and
3. Mapping and interpolation of the SNOWPACK output.

Potential error may arise from the instrumentation because the meteorological parameters that drive the SNOWPACK model can only be measured with a limited degree of accuracy. In most cases, the achieved accuracy is sufficient and should pose no problems; however, two possible exceptions are the measurement of snow depth and snow surface temperature. The effectiveness of the ultrasonic depth gauge is dependent on the calculation of the speed of sound, which varies with temperature. Referring back to Table 6, the snow depths measured with the ultrasonic gauge compare favorably to depths measured on a snow stake and in the snowpits. In a few instances, discrepancies exist but these could be do to the spatial variability of total snowpack depth. The infrared thermometer used to measure the snow surface temperature has a high stated accuracy; while there is no reason to suspect any errors, the instrument has largely been untested on snow.

Human observations have already been discussed at length in previous sections, particularly with regards to determination of snow crystal type and size which are very subjective. The uncertainty in these measurements, along with differing definitions used by the model and field observers, have precluded a robust evaluation of SNOWPACK's ability to predict grain size and shape. The other measurement which is performed manually is density, which can be considered accurate to within the limits of the digital scale and human fallibility.

Possibly the most significant potential for error occurs when the output from SNOWPACK is linearly mapped and then interpolated in order to get model data at the same snowpack depths as the observations. The stretching or shrinking of the simulated snowpack to match the observed one is necessary; however, errors in the modeled settling do not occur linearly through the snow cover depth, but instead are variable and depend on the layer characteristics. Interpolation between nodal data assumes a linear distribution between neighboring elements which is not always present, especially between layers that have dramatically different characteristics. Finally, grain type is not measured on a continuous scale, and thus offers no basis for interpolation. Choosing the grain type nearest the desired location is likely to incur some inaccuracy.

Sources of error are unavoidable in any analysis, and the attempt is always made to limit them as much as possible. Despite the potential inaccuracies outlined above, this evaluation remains the most thorough and objective completed to date. Future work and experience may lead to new methods and techniques that will further improve the precision of the analysis.

Laboratory Investigation

The laboratory experiments were performed primarily to develop techniques for using computed tomography to observe changes in snow microstructure during kinetic-growth metamorphism. As a result, the preliminary results of this investigation will be presented as a demonstration of the methodology, and a detailed analysis of the data will not be given. The following discussion will be based on the results of Experiments 4, which was the most successful. A brief, qualitative discussion of Experiment 3 will also be provided.

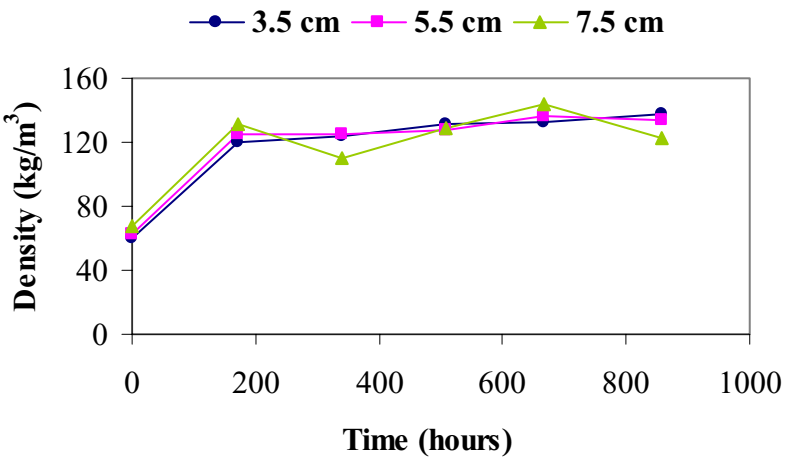

Figure 29. Density variation over time as measured directly from the CT scans. Depth is given as height above the bottom of the cup.

Experiment 4

The fourth experiment was performed with very low density snow composed of new and decomposing precipitation forms (Class 1 and 2a). Using a 4 mm sieve to fill the

sample cups, initial densities near 60 kg/m^3 were still measured from the CT scans (Figure 29), and a density of 63 kg/m^3 was found by weighing the sample cup. A week later, the density at all scan levels had doubled and then experienced little change for the remainder of the experiment. Initially, the cup was filled to 15 cm, but within the first week the snow settled to an average height of 9 cm.

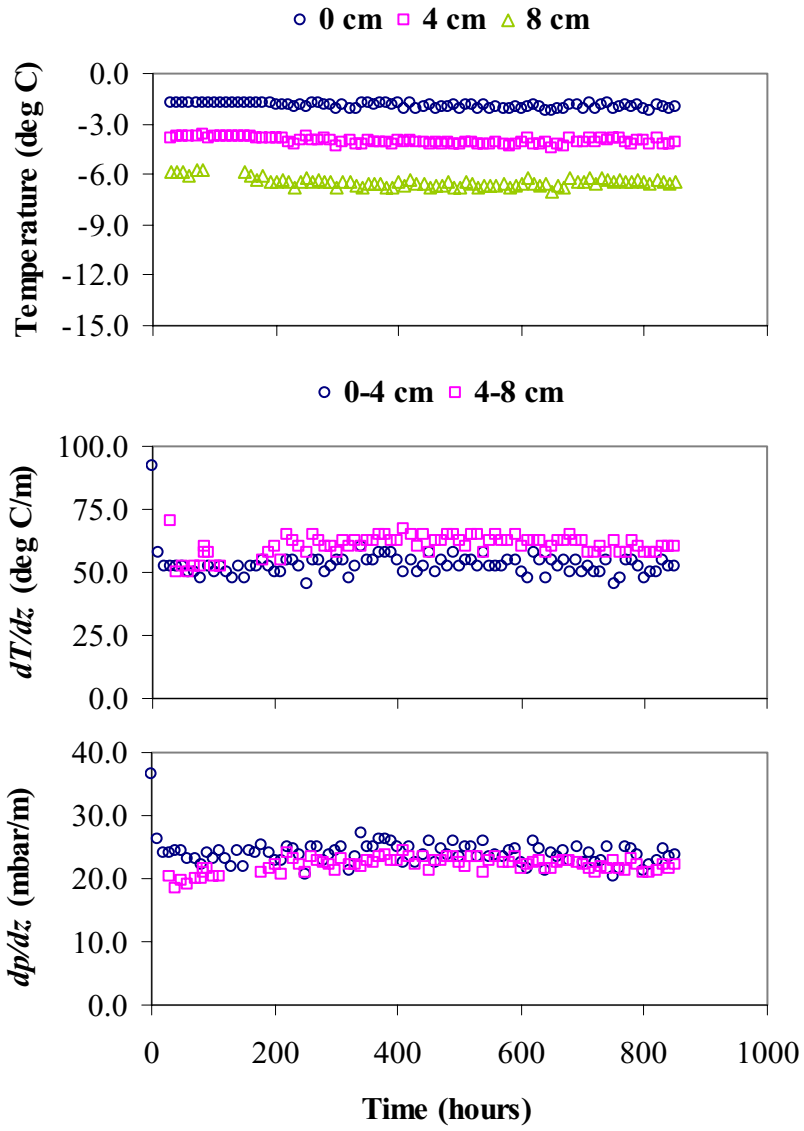

Figure 30. Plots of temperature, temperature gradient, and vapor pressure gradient for Experiment 4.

The temperatures measured over the course of the experiment, as well as the calculated temperature and vapor pressure gradients, are presented in Figure 30. The mean temperature gradient in the snow sample during Experiment 4 was 55 deg C/m. It is evident from this plot that the temperatures remained relatively uniform over the course of the experiment. As a result, there was not much variation in either the temperature or vapor pressure gradients over time. Although the temperature gradient is higher in the upper half (4-8 cm) of the snow sample, the average vapor pressure gradient in the lower portion is still greater due to the warmer temperatures; however, this difference is quite small.

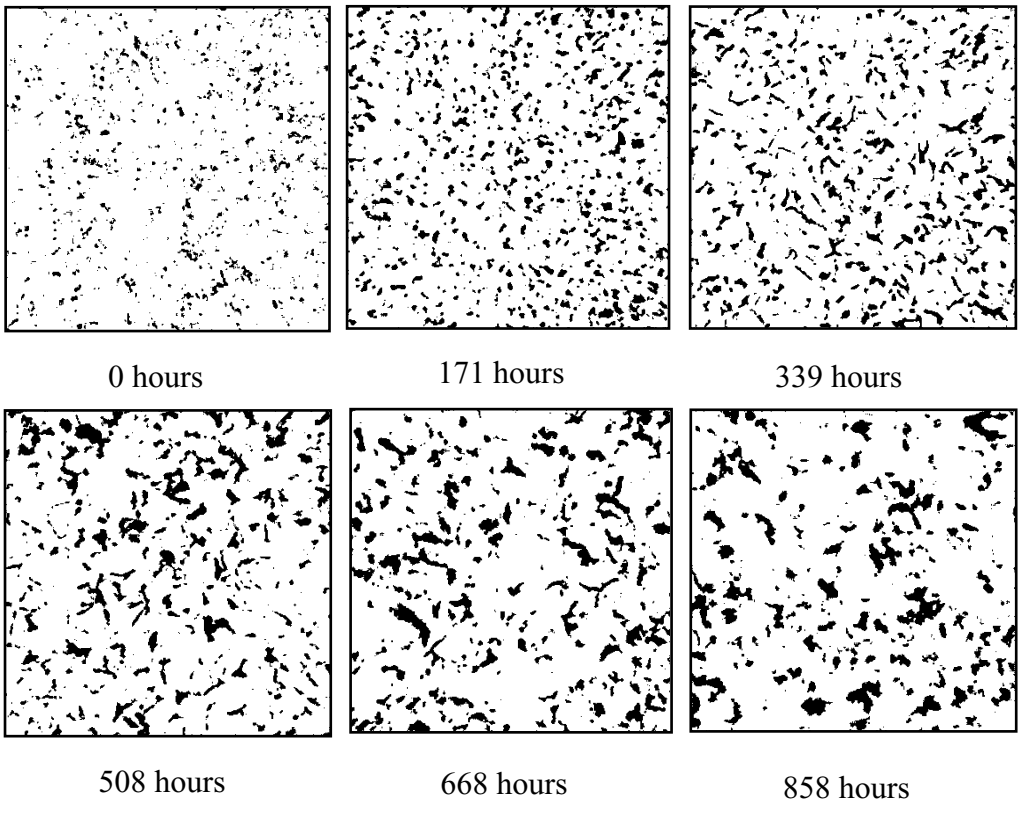

Figure 31. Time series of binary CT images from Experiment 4. Scans were taken from 3.5 cm above the bottom of the sample cup.

As the final step in the experiment, the CT images are converted to binary (Figure 31) and analyzed using the stereological software developed by Edens and Brown (1994). Estimations of grain size are shown in Figure 32. Calculation of the mean grain size using the intercept length method seems to underestimate the grain size, as the crystal sizes observed before and after the experiment were higher than those measured. The volume-weighted-volume (VWV) approach seems to provide a more realistic representation of grain diameter, as the initial grain size is similar to that measured prior to beginning the experiment The small decrease in grain size present during the first week is likely due to the initial breakdown of the precipitation forms.

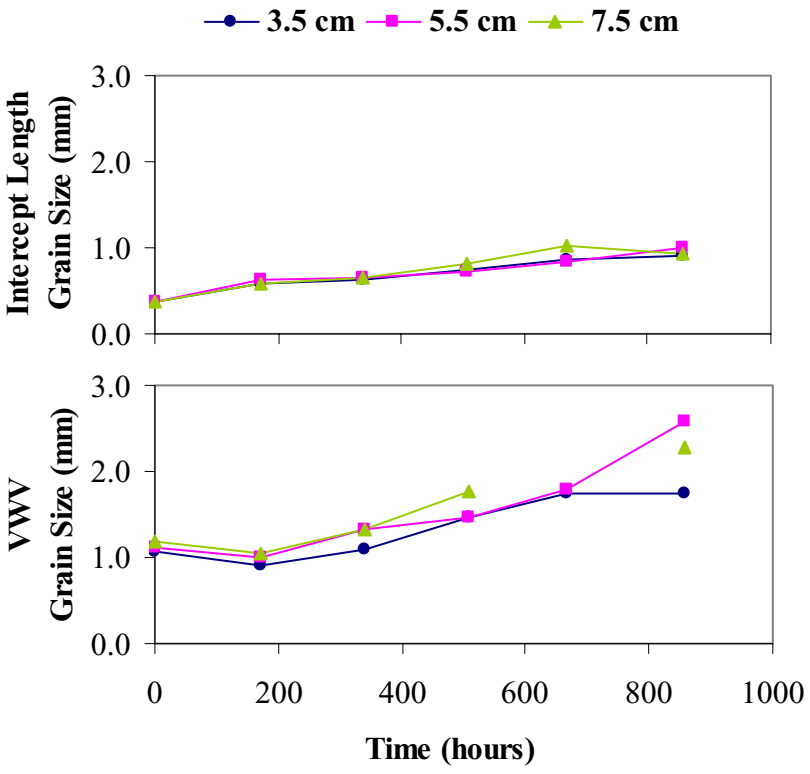

Figure 32. Variation in estimated grain size over time using the intercept line and volume-weighted-volume methods.

Microstructural parameters that describe the intergranular bonding are plotted against time in Figure 33. The size of the bonds is very similar for all three levels, and does not increase greatly during the experiment. The neck length generally increases, but does so

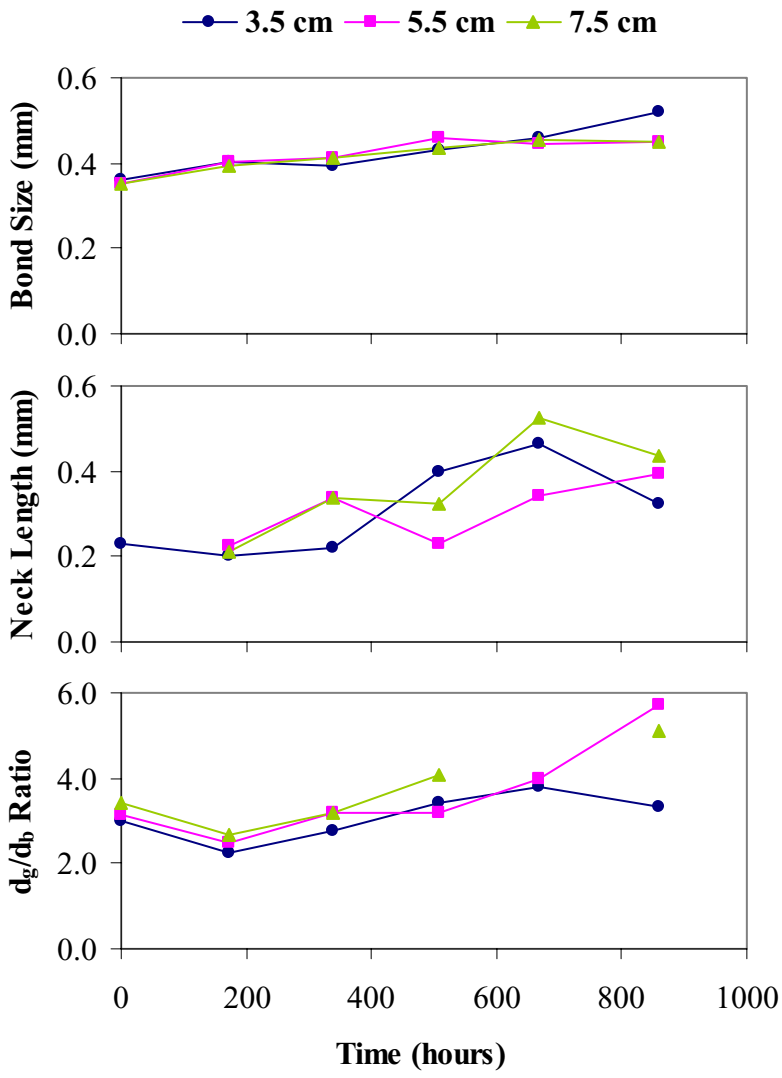

Figure 33. Bond size, neck length, and grain size-to-bond size ratio plotted against time for three different heights above the bottom of the cup.

erratically. During the first week of the experiment, the grain size-to-bond size ratio decreases as the initial precipitation forms break down and bond together. For the remainder of the time period, the ratio steadily increases, implying that within the horizontal plane encompassed by the CT section, grain growth outpaces the building of bonds. This behavior is common during kinetic-growth metamorphism and accounts for the weakness of the associated faceted crystals. However, no conclusions can be drawn pertaining to the bonds in the vertical direction, which are typically much more developed in advanced stages of faceted snow.

An important observation is that, for a given time, there is very little variation in the properties of the snow among the different height levels. A reasonable explanation of this is provided in Figure 30: over the course of the experiment, the average vapor pressure gradient throughout the sample cup is relatively constant. Therefore, the degree of metamorphism occurring within the snow specimen should also be uniform.

Experiment 3

In this experiment, manufactured ice balls of approximately uniform diameter (7-8 mm) were subjected to a large temperature gradient averaging 65 deg C/m. While the density of the sample was high (Figure 34), sufficient pore space was present to allow the transfer of water vapor. The initial density, measured by weighing the sample, was 543 kg/m^3, and the average density calculated from the first CT images was 584 kg/m^3. Incidentally, these values correspond well with the theoretical density of random close-packed spheres which is approximately 587 kg/m^3, based on a hypothetical 64% volume

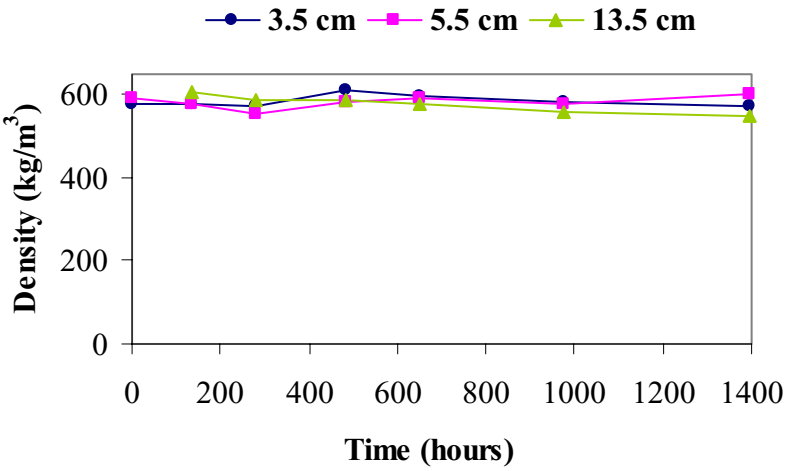

Figure 34. Variation in density over time as measured from the CT scans. Level is given as height above the bottom of the sample cup.

fraction. One of the motivations behind performing this experiment was to determine whether the mass transfer occurring during metamorphism would cause a measurable increase or decrease in the density at different levels within the sample cup. However, it is evident from Figure 34 that little change occurs in the measured density over the course of the experiment.

Binary CT images taken during the experiment are shown in Figure 35. While the driving mechanisms are the same as for natural snow, applying a large temperature gradient to the manufactured ice balls gives very different results. In general, the grains tend to shrink as mass is removed through sublimation, and the resulting vapor recrystallizes onto other spheres causing formations having an appearance similar to surface hoar. Unfortunately, the feathery growth in the pore space between the spheres prevented the stereology software from making accurate measurements of the microstructure.

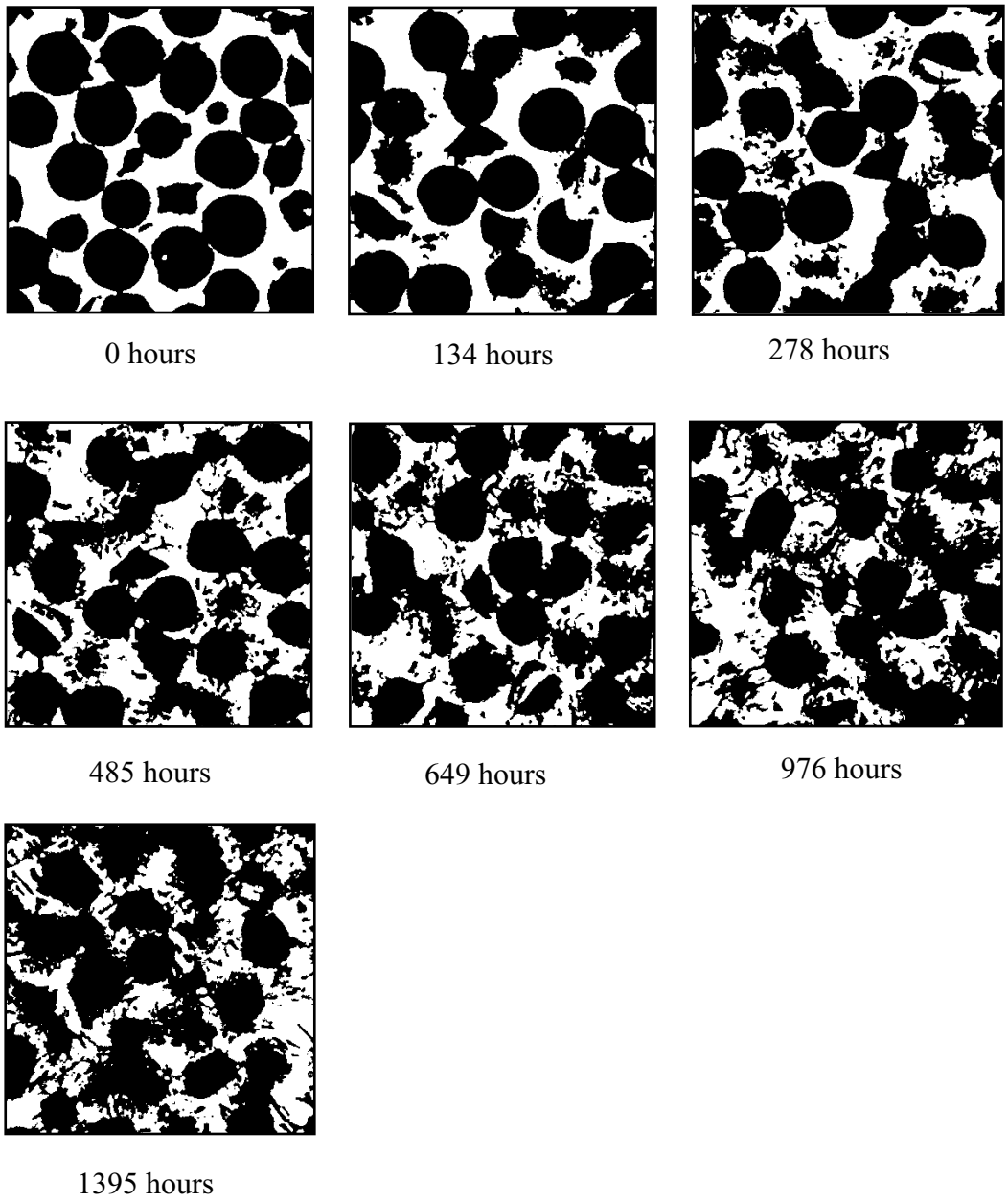

Figure 35. Time series of binary CT images from Experiment 3. Scans were taken 5.5 cm above the bottom of the sample cup.

CHAPTER 5

CONCLUSIONS AND RECOMMENDATIONS

Field Investigation

From 17 November 1999 to 6 April 2000, meteorological data were collected from a mountain weather station adjacent to Bridger Bowl Ski Area near Bozeman, MT. During the same period, full snowpack profiles were performed on a weekly basis within a short distance from the weather station. By running the SNOWPACK model using the collected weather data and comparing the output to the snow profiles, a thorough evaluation of the predictive capabilities of the model was possible. Statistical tests were utilized to make the comparison as objective as possible.

The results of several statistical tests indicate that the SNOWPACK model predicts the temperature profile within the snow cover quite accurately. This aspect of the program is crucial since the majority of the processes occurring within the snowpack have a strong temperature dependence. Since the accuracy of the temperature prediction diminishes slightly in the uppermost region of the snowpack, improvements in the manner SNOWPACK models the surface energy exchanges may be necessary. The snow surface albedo, for instance, governs the fraction of shortwave radiation that is absorbed into the snow cover, affecting snow temperature as well as many snowpack processes which are temperature-dependent. Additional difficulties are encountered in the

springtime when the regions of snowpack becomes isothermal; in this scenario SNOWPACK does not always allow the snow cover to refreeze and hence the temperatures will not drop below freezing. This aspect of the model may improve as the wet snow metamorphism routine becomes more sophisticated.

Temperature gradient is a secondary quantity which must be numerically differentiated from temperature, so the statistical accuracy of the modeled temperature gradient compared to the measured counterpart should be reduced. Despite this fact, the statistical tests yielded much lower results than would be expected given the accuracy with which snowpack temperatures are predicted by the model. Since the measured temperature gradient must also be calculated, the comparison of two secondary quantities could explain the unexpectedly poor results. The number of outlying data points indicate the need to analyze the data in an alternate manner, possibly by comparing small and large temperature gradients, or those found in the upper and lower snowpack, independently.

While the magnitude of the snowpack density is not predicted very successfully, SNOWPACK is able to follow the trends fairly closely. When snowfall occurs, the model consistently overpredicts the density of the new precipitation. Since the routine that determines new snow density is empirical in nature, additional data and adjustment of the relation may improve this aspect of the model, or perhaps the empirical equation is biased towards the climatic conditions present in Switzerland. An alternative would be to require that the snow water equivalency of the new snowfall be measured at the weather station. Estimation of the new snow density is crucial as it provides a starting point for

proceeding density calculations, and alters the mass balance of the snowpack. Once the snowfall has been added to the snowpack, SNOWPACK typically predicts a viscosity that is too high, resulting in consistent underprediction of the snowpack density. Because the viscosity model has been validated, some other source of error seems more plausible. One possibility is the calculation of grain and bond size, on which the viscosity is strongly dependent. The metamorphism laws that govern these parameters are largely unproven and may require refinement.

A meaningful comparison of predicted and observed grain size is difficult due to different definitions of grain size and the subjectivity of human measurement. The statistical measures generally gave poor results and indicate little correlation between the simulated and observed values. The measures did not improve much when the grain size was normalized according to the minimum and maximum grain size. While the model computes grain size independent of the crystal shape, the human observer has a difficult time separating the two. This results in a frequent overestimation of grain size by snow practitioners, especially when the crystals are irregular in shape. Therefore, the results of the comparison may not indicate the need to improve the model, but rather the utility of a more standardized observation technique using a definition of grain size similar to that employed by SNOWPACK.

The comparison of predicted and observed crystal shape is even more troublesome than for grain size since crystallography is not measured on a continuous or numeric scale. This requires the use of an alternative statistical measure that is not as robust as those utilized for the above parameters. The results of the statistical test demonstrated a

low correlation between the modeled and observed grain types, but a proprietary measure developed by Lehning et al (2000) yielded a more optimistic agreement. Like grain size, crystal shape is a very subjective observation, but in this case the problem seems to lie in the model's determination of crystallography. SNOWPACK relies on the grain type indicators sphericity and dendricity, which are somewhat arbitrary in nature and difficult to physically measure, especially in the field. Furthermore, the change in these parameters due to equilibrium or kinetic-growth metamorphism is based on empirical relationships. In order to effectively model the grain type, a classification scheme that is both measurable and has some physical basis would be a tremendous advantage, as it could be predicted using a theoretical rather than empirical formulation. Fierz and Baunach (2000) have made some progress in this area with their development of "zero curvature", but it is unclear how this parameter could be incorporated into a physical model. Improvement of the grain type prediction capability of SNOWPACK is of paramount importance since it plays such a significant role in the stratification, strength, and stability of the snowpack.

Currently, SNOWPACK has only rudimentary provisions for simulating wet snow metamorphism. In several instances, the model predicted surface melting at appropriate times, but tended to predict thick layers of wet grains when only thin melt-freeze crusts were observed. The ability of the model to predict when these wet grains refreeze also needs to be improved, as this has an effect on the temperature and strength of the snow. Future work on the wet snow capabilities of SNOWPACK will be important for ablation

prediction, hydrological purposes, and for applying the model to warmer, maritime climates.

Additional work is also necessary to improve SNOWPACK's ability to predict the occurrence and development of surface hoar. At the present time, the model seems to simulates surface hoar on most occasions when it actually occurs, but also predicts it in several instances where surface hoar did not form. Since surface hoar can be such a dangerous weak layer in the alpine snowpack, accurate prediction of its formation and properties will greatly increase the utility of the SNOWPACK model.

Since a certain amount of error is inherent in the analysis methodology, improvement of the techniques presented herein could permit a more accurate comparison of the model output to field data. The settlement errors do not vary linearly through the depth of the snowpack, so a more suitable procedure for stretching or shrinking the modeled snowpack to match the observed depth seems appropriate. Performing the statistical tests independently for early-winter, mid-winter, and spring data would isolate the performance of SNOWPACK during these periods. In addition, a quantitative appraisal of instrumentation error would verify whether certain model variables are predicted within the limits of measurement accuracy. Finally, validation of any model is an ongoing process which becomes increasingly effective with additional data. Each winter season and geographic location is unique and will provide further insight into the successes and flaws of the SNOWPACK model.

In its present form, the SNOWPACK model can be a useful tool to avalanche forecasters and other practitioners who desire to know the properties and structure of the

snow cover, but do not always have the ability to conduct frequent snow profiles in a given location. While users of the model should understand the limitations of the current version of SNOWPACK and not place absolute faith in the output, they should also recognize that it provides sufficient accuracy to offer a valuable supplement to many traditional avalanche and snow programs. Future work, in the form of validation and model improvements, will increase the overall accuracy of SNOWPACK and its prevalence as a tool for snow practitioners world-wide.

Laboratory Investigation

A laboratory study was conducted to develop techniques to measure the changes in microstructure of snow subjected to the large temperature gradients that drive kinetic-growth metamorphism. While similar experiments have been performed in the past, applications of new technologies and methods presents a renewed opportunity for making more accurate and detailed measurements.

Snow samples were subjected to strong temperature gradients in a cold-room laboratory over a period of about one month. The temperature gradients were typically 50-65 deg C/m and resulted in vapor pressure gradients in excess of the 5 mbar/m threshold required for kinetic-growth metamorphism to occur (Armstrong, 1985). On a weekly basis, the same snow sample was CT scanned at three different heights to obtain horizontal, cross-sectional images at these levels. After the CT images were converted to

binary, they were analyzed with an innovative software that measures the microstructure of the snow automatically and objectively.

The results of the microstructural measurements for Experiment 4 show an increase in grain size, bond size, and neck length at all scan heights; however, the grain growth far outpaces the increase of the other quantities. Densities at all levels initially increased due to settlement, then remained relatively constant throughout the remainder of the experiment.

Experiment 3 was performed using man-made ice spheres. While the transference of water vapor was apparent as crystalline formations developed in the pore space, no significant changes in density occurred as a result of the mass flux.

The methodology presented provides a powerful tool for examining metamorphic processes within snow. The use of CT technology allows nondestructive sampling of a snow specimen, so that the internal structure of a single snow sample can be repeatedly observed over time. This technique eliminates errors due to spatial variation and is a less time-consuming (albeit more expensive) alternative to surface sectioning. Utilization of a specialized stereology software package provides an objective, consistent, and efficient means for collecting a variety of information pertaining to the small-scale properties of snow.

Constructing a dedicated cold chamber that keeps a snow sample cold indefinitely would allow many more CT scans to be performed at many different heights within the sample. Performing numerous, closely-spaced scans would also be possible, which would permit a three-dimensional reconstruction of the snow microstructure. By repeating the

experiment for many different temperature gradients, snow types, and densities, a comprehensive database could be developed that would provide valuable information regarding the changes in snow microstructure under many different conditions. In turn, this data could be applied towards the validation of present metamorphism models and the development of new theories.

REFERENCES CITED

REFERENCES CITED

Adams, E. E. and Brown, R. L. 1982. Further results on studies of temperature gradient metamorphism. *J. Glaciology 18(98),* 205-210.

Adams, E. E. and Brown, R. L. 1983. Metamorphism of dry snow as a result of temperature gradient and vapor density differences. *Ann. Glaciology 4*, 3-9.

Adams, E. E. and Brown, R. L. 1989. A constitutive theory for snow as a continuous multiphase mixture. *International J. Multiphase Flow 15(4),* 553-572.

Adams, E. E. and Brown, R. L. 1990. A mixture theory for evaluating heat and mass transport in nonhomogenous snow cover. *J. Continuum Mechanics and Thermodynamics 2*, 31-63.

Adams, E. E. and Sato, A. 1993. Model for effective thermal conductivity of a dry snow cover composed of uniform ice spheres. *Ann. Glaciology 18*, 300-304.

Akitaya, E. 1967. Some experiments on the growth of depth hoar, in Physics of Snow and Ice, Pt. 2. *Proc. Sapporo Conf.,* Inst. Low Temp. Sci., 713-723.

Akitaya, E. 1974. Studies on depth hoar. *Contrib. Inst. Low Temp. Sci*., *Ser. A, 26*. 67 pp.

Armstrong, R. L. 1985. Metamorphism in a subfreezing, seasonal snow cover: The role of thermal and vapor pressure conditions. Ph.D. dissertation. Department of Geography, University of Colorado. 175 pp.

Bader, H. and Colleagues. 1939. *Der schnee und seine metamorphose*. Snow, Ice, and Permafrost Research Establishment, U.S. Army, 313 pp.

Bader, H. P. and Weilenmann, P. 1992. Modeling temperature distribution, energy and mass flow in a (phase-changing) snowpack. I. Model and case studies. *Cold Regions Sci. Tech. 20*, 157-181.

Bartelt, P., Lehning, M., and Brown, R. L. 2000. A physical model for the Swiss avalanche warning service. Part I: Numerical model. In preparation.

Birkeland, K. W. 1998. Terminology and predominant processes associated with the formation of weak layers of near-surface facet crystals in the mountain snowpack. *Arctic Alpine Res. 30(2)*, 193-199.

Birkeland, K. W., Johnson, R. F., and Schmidt, D. S., 1998: Near-surface faceted crystals formed by diurnal recrystallization: a case study of weak layer formation in the mountain snowpack and its contribution to snow avalanches. *Arctic Alpine Res*. *30(2),* 200-204.

Box, G. E. P., Hunter, W. G., and Hunter, J. S. 1978. *Statistics for Experimenters*. John Wiley and Sons, New York.

Bradley, C. C., Brown, R. L., and Williams, T. 1977. On depth hoar and the strength of snow*. J. Glaciology 18(78),* 145-147.

Bradley, C. C., Brown, R. L., and Williams, T. 1977. Gradient metamorphism, zonal weakening of the snowpack, and avalanche initiation. *J. Glaciology 19(81),* 335-342.

Brown, R. L., Adams, E. E., and Barber, M. 1994. Non-equilibrium thermodynamics applied to metamorphism of snow. *Proc. Snowsymp 94*, 39-50.

Brown, R. L., Edens, M. Q., and Barber, M. 1999. Mixture theory of mass transfer based upon microstructure. *Defense Science J. 49(5),* 393-409.

Brun, E., Martin, E. Simon, V., Gendre, C., Coleou, C. 1989. An energy and mass model of snow cover suitable for operational avalanche forecasting. *J. Glaciology 35(121)*, 333-342.

Brun E. P., David, P., Sudul, M., and Brugnot, G. 1992. A numerical model to simulate snowcover stratigraphy for operation avalanche forecasting. *J. Glaciology 38(128),* 13-22.

Christon, M., Burns, P., Thompson, E., and Sommerfeld, R. 1987. Water vapor transport in snow, a 2-d simulation of temperature gradient metamorphism. *Seasonal Snowcovers: Physics, Chemistry, Hydrology*, edited by G. Jones and W. J. Orville-Thomas, D. Reidel Publishing Company, 37-62.

Christon, M., Burns, P. J., and Sommerfeld, R. A. 1993. Quasi-steady temperature gradient metamorphism in idealized, dry snow. *Numerical Heat Transfer*, 1-29.

Colbeck, S. C. 1980. Thermodynamics of snow metamorphism due to variations in curvature. *J. Glaciology 26(94),* 291-301.

Colbeck, S. C. 1983. Theory of metamorphism of dry snow. *J. Geophysical Res 88(C9)*, 5475-5482.

Colbeck, S. C. 1987. Snow metamorphism and classification. *Seasonal Snowcovers: Physics, Chemistry, Hydrology*, edited by G. Jones and W. J. Orville-Thomas, D. Reidel Publishing Company, 1-35.

Colbeck, S. C, Akitaya, E., Armstrong, R., Gubler, H., Lafeuille, K., Leid, D., McClung, D., and Morris, E. 1990. The international classification for seasonal snow on the ground. *International Commission on Snow and Ice*, 23 pp.

Colbeck, S. C. 1991. The layered character of snow covers. *Rev. Geophysics 29(1)*, 81-96.

Coleou, C. Lesaffre, B., Brzoska, J., Ludwig, W., and Boller, E. 2000. *Proc. International Symp. Snow and Avalanches*, Innsbruck, Austria, in press.

Dixon, W. J. and Massey, Jr., F. J. 1983. *Introduction to Statistical Analysis, Fourth Edition*. McGraw-Hill Book Company.

de Quervain, M. 1963. On the metamorphism of snow. *Ice and Snow: Properties, Processes, and Applications*, edited by W. D. Kingery, MIT Press, Cambridge, Mass., 377-390.

Durand, Y., Giraud, G., Brun, E., Merindol, L., and Martin, E. 1999. A computer-based system simulating snowpack structures as a tool for regional avalanche forecasting. *J. Glaciology 45(151),* 469-484.

Edens, M. Q. and Brown, R. L. 1994. Measurement of microstructure from surface sections. *Proc. Snowsymp 94*, 63-72.

Ehrenberg, A. S. C. 1982. *A Primer in Data Reduction*. John Wiley and Sons, England.

Eugster, H. P. 1952 Beitrag zu einer Gefugeanalyse des Schnees. *Beitr. Geol. Schweiz, Geotech. Ser. Hydrologie*, Kummerly u. Frey, Bern.

Fierz, C. and Baunach, T. 1999. Quantifying grain shape changes in snow subjected to large temperature gradients. *Ann. Glaciology 31*, in press.

Giddings, J. C. and LaChapelle, E. 1962. The formation rate of depth hoar. *J. Geophysical Res. 67(6)*, 2377-2382.

Gray, J. M. N. T. and Morland, L. W. 1994. A dry snow pack model. *Cold Regions Sci. Tech. 22*, 135-148.

Gubler, H. 1978. An alternate statistical interpretation of the strength of snow. *J. Glaciology 20(83),* 343-357.

Gubler, H. 1985. Model for dry snow metamorphism by interparticle vapor flux. *J. Geophysical Res. 90(C8),* 8081-8092.

Hansen, A. C. and Brown, R. L. 1986. The granular structure of snow: an internal-state variable approach. *J. Glaciology 33(112),* 434-438.

Jordon, R. 1991. A one-dimensional temperature model for a snow cover. *CRREL Report 91-16.*

Kawamura, T. 1990. Nondestructive, three-dimensional density measurements of ice core samples by x ray computed tomography. *J. Geophysical Res. 95(B8),* 12,407-12,412.

Kry, P. R. 1975. Quantitative stereological analysis of grain bonds in snow. *J. Glaciology 14(72),* 467-477.

Lehning, M., Bartelt, P., Brown, R. L., Russi, T. Stockli, U., and Zimmerli, M. 1998. A network of automatic weather and snow stations and supplementary model calculations providing snowpack information for avalanche warning. *Proc. 1998 International Snow Sci. Workshop*, Sun River, Oregon, 225-233.

Lehning, M., Bartelt, P., Brown, R. L., Russi, T. Stockli, U., and Zimmerli, M. 1999. SNOWPACK model calculations for avalanche warning based upon a new network of weather and snow stations. *Cold Regions Sci. Tech. 30*, 145-157.

Lehning, M. Brown, R. L., Bartelt, P., Fierz, C., and Satyawali, P. 2000a. A physical model for the Swiss avalanche warning service. Part II: Snow microstructure, meterological boundary conditions, and applications. In preparation.

Lehning, M., Fierz, C., and Lundy, C. 2000b. An objective snow profile comparison

method. *Proc. 2000 International Snow Sci. Workshop*, Big Sky, Montana, submitted.

List, R. J. 1949. *Smithsonian Meteorological Tables*. 6th revised ed. Smithsonian Miscellaneous Collections 14(104). Smithsonian Institution, Washington, D.C., 350-364.

Lundy, C. and Adams, E. E. 1998. Nondestructive collection of natural snow specimens for use with CT scan analysis. *Proc. 1998 International Snow Sci. Workshop*, Sun River, Oregon, 208-213.

Mahajan, P. and Brown, R. L. 1993. A microstructure-based constitutive law for snow. *Ann. Glaciology 18*, 287-294.

Marbouty, D. 1980. An experimental study of temperature-gradient metamorphism. *J. Glaciology 26(94),* 303-312.

McClung, D. and Schaerer, P. 1993. *The Avalanche Handbook*. The Mountaineers, Seattle, Washington. 271 pp.

Mellor, M. 1977. Engineering properties of snow. *J. Glaciology 19(81),* 15-66.

Morland, L. W., Kelly, R. J., and Morris, E. M. 1990. A mixture theory for a phase-changing snowpack. *Cold Regions Sci. Tech. 17*, 271-285.

Paulke, W. 1934. Der Schnee und seine Diagenese. *Z. Gletscherkunde XXI*, 259-282.

Perla, R. I. And Martinelli, Jr., M. 1976. *Avalanche Handbook*. U.S. Department of Agriculture, Forest Service, Agriculture Handbook 489.

Perla, R. 1978. Temperature-gradient and equi-temperature metamorphism of dry snow. *Proc. International Meeting on Snow and Avalanches 12-13*, 1978, Grenoble, 43-48.

Perla, R., Dozier, J. and Davis, R. E. 1986. On the objective analysis of snow microstructure. Draft of paper presented at Davos symposium, 1986. 16 pp.

Pielmeier, C., Schneebeli, M., and Stucki, T. 2000. Snow texture: a comparison of empirical versus simulated texture index of snow. In preparation.

Satyawali, P. K., Brown, R. L., and Scheebeli, M. 1999. Role of temperature gradient metamorphism during snowpack evolution. *J. Glaciology*, submitted.

Seligman, G. 1936. *Snow Structure and Ski Fields. Macmillan*, London. 555 pp.

Siegel, S. and Castellan Jr., N. J. 1988. *Non-parametric Statistics for the Behavioral Sciences, 2nd Edition*.

Snedecor, G. W. and Cochran, W. G. 1989. *Statistical Methods, Eighth Edition*. Iowa State University Press, Ames, Iowa.

Sommerfeld, R. A. 1983. A branch grain theory of temperature gradient metamorphism in snow. *J. Geophysical Res. 88(C2),* 1484-1494.

Trabant, D., and Benson, C. 1972. Field experiments on the development of depth hoar*. Mem. Geological Soc. Am. 135*, 309-322.

Weibel, E. R. 1980. *Stereological Methods, Volume 2: Theoretical Foundations*. Academic Press, New York and London.

Yen, Y. C. 1981. Review of thermal properties of snow, ice, and sea ice. *CRREL Rep. 81-10.*

Yosida, Z., and Colleagues. 1955. Physical studies on deposited snow, I, Thermal properties. *Contrib. Institute Low Temp. Sci. 7, 10-74*.

APPENDIX

DEFINITION OF ISCI SNOW CLASSIFICATION SYMBOLS

Symbol	Class	Description
+	1	Precipitation particle
/	2	Decomposing precipitation particle
l	3	Rounded grain
¤	4	Faceted crystal
l¤	3c, 4c	Mixed forms
Λ	5	Depth hoar
¡	6	Wet Grain
V	7	Surface hoar

(Colbeck et al, 1990)